NASA CONTRACTOR REPORT

NASA CR-1031

OPTICAL ABSORPTION IN FUSED SILICA DURING TRIGA REACTOR PULSE IRRADIATION

by R. Gagosz, J. Waters, F. C. Douglas, and M. A. DeCrescente

Prepared by
UNITED AIRCRAFT CORPORATION
East Hartford, Conn.
for

NATIONAL AERONAUTICS AND SPACE ADMINISTRATION • WASHINGTON, D. C. • APRIL 1968

OPTICAL ABSORPTION IN FUSED SILICA DURING TRIGA REACTOR PULSE IRRADIATION

By R. Gagosz, J. Waters, F. C. Douglas,
and M. A. DeCrescente

Issued by Originator as Report No. F-910485-1

Prepared under Contract No. NASw-847 by
UNITED AIRCRAFT CORPORATION
East Hartford, Conn.

for

NATIONAL AERONAUTICS AND SPACE ADMINISTRATION

For sale by the Clearinghouse for Federal Scientific and Technical Information
Springfield, Virginia 22151 – CFSTI price $3.00

Optical Absorption in Fused Silica during TRIGA Reactor Pulse Irradiation

TABLE OF CONTENTS

Optical Absorption in Fused Silica during TRIGA Reactor Pulse Irradiation

SUMMARY

An experimental investigation was conducted to determine the spectral transmission characteristics of fused silica before, during and after exposure to reactor irradiation pulses. The transmission measurements were carried out at three wavelengths (0.215, 0.625 and 1.0 microns) and at a range of temperatures from ambient to 900°C. Corning 7940 fused silica specimens in a corner cube configuration were mounted next to the reactor core face of the University of Illinois' TRIGA Mark II reactor. Peak neutron and gamma fluxes obtained from this reactor were approximately 5.4×10^{15} n/cm^2-sec and 6.1×10^{7} R/sec, respectively. Neutron and gamma doses associated with these pulses were 2.3×10^{14} n/cm^2 and 2.6×10^{6} R, respectively. The effective time of the pulse obtained by dividing the total dose by the peak flux was approximately 0.043 sec. The transmission measurements were made immediately before, during and after the reactor pulses to monitor both the creation of irradiation induced absorption and the decay of the induced absorption after the pulse.

RESULTS

1. Ambient-temperature pulse irradiation studies at wavelengths of 1.0 to 1.1 microns in the infrared indicate no induced absorption in the specimen.

2. Pulse irradiation studies at a wavelength of 0.625 microns in the visible indicate that:

a) less than 0.01 cm^{-1} of absorption is induced by the irradiation; and

b) at a specimen temperature of 500°C, the bleaching (color removal) of the irradiation-induced absorption is complete in less than 1 second.

3. Pulse irradiation studies at a wavelength of 0.215 microns in the ultraviolet at ambient specimen temperatures indicate that:

a) no transient absorption (color present only during the neutron pulse) occurs, since the growth of absorption during the pulse is a smooth variation with time;

b) nearly 50% of the absorption induced by the irradiation pulse is bleached at room temperature during the 20 minutes between pulses; and

c) defects may be completely removed by subsequent annealing at temperatures between 508°C and 862°C.

4. Interpretation of the results of elevated-temperature pulse irradiation studies at a wavelength of 0.215 microns in the ultraviolet was hampered by an indicated negative absorption during the pulse which was not present at lower temperatures and which could have been caused by fluorescence from the specimen. However, measurements made immediately after the pulse indicated that:

a) the induced absorption created per pulse is on the order of 0.07 cm^{-1};

b) the rate of decay of this absorption is faster at the higher temperatures, the bleaching time constant being approximately 0.3 seconds at 900°C and 0.5 seconds at 500°C (this bleaching time constant is approximately two orders of magnitude less than bleaching time constants determined from post-reactor measurements); and

c) the calculated equilibrium absorption at a continuous neutron flux equal to the peak transient neutron flux in the tests is approximately 0.7 cm^{-1} for a specimen temperature of 900°C. This calculated equilibrium absorption coefficient is proportional to the decay time constant, and, hence, is less than that indicated from post-reactor measurements of decay time constant.

INTRODUCTION

A program is being conducted at the Research Laboratories of United Aircraft Corporation under Contract NASw-847 with the Joint AEC-NASA Space Nuclear Propulsion Office to determine the feasibility of the nuclear light bulb rocket engine concept. This engine concept is based on the transfer of energy by thermal radiation from gaseous nuclear fuel through an internally cooled transparent wall to seeded hydrogen propellant. This concept requires that the transparent wall in the engine remain transparent when subjected to the intense neutron and gamma irradiation from the nuclear fuel. The program described in the present report is one of three programs which have been conducted to obtain information on nuclear irradiation effects in candidate wall materials. The other two programs have relied on transmission measurements which have been made after the transparent materials have been removed from the reactor, and are described in Refs. 1 and 2. Information on the transmission characteristics of unirradiated specimens is contained in Ref. 3 as well as in Refs. 1 and 2.

Examination of the transmission characteristics of optical materials following a nuclear reactor irradiation can be used to obtain valuable information regarding the long-lived neutron-induced damage sites produced during the irradiation process. These measurements may not, however, provide any information regarding the equilibrium absorption associated with short-lived damage sites present during the irradiation process, because annealing of neutron induced damage may occur during the cool-down cycle following the irradiation. In addition, the specimens receive a finite gamma irradiation dose from the radioactive capsule used to contain the specimens during the irradiation, thereby increasing the measured absorption (Ref. 2). Carefully controlled irradiations reduce the amount of uncertainty in these experiments, but still do not yield exact information concerning the absorption present during the irradiation process due to short-lived damage sites.

A program was initiated at the United Aircraft Research Laboratories to examine the absorption present in an optical material, specifically fused silica, during the irradiation process. The first part of the program was the development of the optical and electronic instrumentation required to perform the experiment in a radiation environment. The second part of the program was the experimental investigation performed at the University of Illinois' TRIGA Mark II reactor. Measurements of the optical transmission characteristics of fused silica were made at 0.215, 0.625 and 1.0 microns immediately before, during and after TRIGA irradiation pulses. Temperatures of the fused silica specimens ranged between ambient and 900°C.

DESCRIPTION OF EQUIPMENT

System Configuration

The optical instrument developed for the in-reactor studies is capable of making transmission measurements during the TRIGA pulse at any selected wavelength from 0.21 to 1.1 microns and at specimen temperatures ranging from ambient to 900°C with an overall response time of 3 milliseconds and to an accuracy of ±5%. A schematic diagram of the optical configuration of the instrument is presented in Fig. 1. As indicated in the figure, optical radiation, selected from either of two light sources, passes through a condensing system which serves to collect the radiation and focus it on a variable aperture which acts as a point source for the collimating optics. The light is then collimated using an off-axis parabolic first surface mirror (Perkin-Elmer 098-0041) and directed towards the specimen located in the nuclear environment using a 45° prism silvered on the two perpendicular faces. A variable field stop is present in the collimating system in order to limit the amount of light received by the specimen. The specimen itself is a corner cube prism made of Corning 7940 U.V. grade fused silica and is mounted within a water cooled furnace assembly located at the internal end of the beam port next to the reactor core face. In traversing the specimen, the light is internally reflected such that it is redirected out of the nuclear environment parallel to, but laterally displaced from, the incoming beam (an inherent characteristic of the corner cube configuration). The light then strikes the second silvered face of the 45° prism and is directed towards a second off-axis parabolic mirror (Perkin-Elmer 098-0041) which focuses the light on the entrance slit of the monochromator (Perkin-Elmer 99) and detector subsystem via an auxiliary first surface mirror. In order to obtain rapid data acquisition of transient effects, a Visicorder, equipped with 500 KC galvanometers, is employed to record the output from the detector subsystem.

Different light sources and detector combinations can be used to cover the various regions of the optical spectrum. However, during any one reactor pulse, the transmission measurement is restricted to a single wavelength since the transient pulses of nuclear radiation produced by the TRIGA reactor are on the order of 180 milliseconds duration with a half peak power width of only 30 milliseconds. Three regions are of primary interest for the in-reactor tests. The first two are the regions around 0.215 and 0.625 microns where irradiation-induced absorption bands are located as indicated by earlier post-reactor annealing experiments. The third region is at 1.0 microns where theory indicates that absorption might be created by the presence of free electrons in the specimen. The light sources and detectors were chosen to insure that a sufficient amount of radiant energy is present in these regions.

For the region around 0.215 microns, the Hanovia 771-B-32 hydrogen discharge lamp was chosen in combination with a modified Cary 1P28 photomultiplier detector.

The hydrogen discharge lamp with two permanently mounted Suprasil windows provides ample energy in the ultraviolet down to 0.16 microns (85% transmission at 0.18 microns). The 1P28 photomultiplier tube, modified with an extremely thin entrance window, provides ample signal down to 0.20 microns.

For the 0.625 and 1.0 micron regions a tungsten ribbon filament lamp (18A/T10/1P-6V) having a brightness temperature of 2200°C is used in conjunction with a 7102 photomultiplier tube. The tungsten ribbon lamp was selected over a Nernst glower due to the tungsten lamp's higher energy output at 1.0 micron (approximately four times greater). The 7102 photomultiplier has sufficient response out to 1.1 microns.

In addition to the limitation of one spectral region per pulse, the relatively short nuclear radiation pulse also imposes a limitation on the instrument operating mode; the detector subsystem cannot be operated in an optically chopped mode. This in turn necessitates d-c operation of the light sources in order to present a non-varying signal to the detectors. The major problem created by this requirement is in the power supply for the hydrogen discharge lamp which is normally run in an a-c mode. A special current-regulated (±2%) power supply was fabricated which is capable of 2 kilovolts to 3.5 kilovolts output at a current rating of 0.2 amps to 0.5 amps. This degree of current regulation (±2%) restricts the light intensity variation to ±4% which is within the noise level of the overall system.

Furnace Design

For the purpose of making tests at elevated specimen temperatures, a water cooled furnace was fabricated. The furnace assembly is composed of alundum ceramic wrapped with nichrome wire which in turn is wrapped with insulation. This entire assembly was contained within a water jacket in order to remove any possibility of the furnace damaging the reactor beam port from excessive heating. A closed circulating water system is used in connection with a heat exchanger to transfer any heat accumulation out of the system. In this way any radiation hazard due to contaminants which might be formed in the nuclear environment is minimized. A platinum-platinum-13-percent rhodium thermocouple was located within the furnace in the immediate vicinity of the sample position to monitor both sample and furnace temperatures. This furnace assembly was capable of maintaining a sample temperature anywhere between ambient and 900°C.

Specimen Configuration

Since the reactor has no through port which passes next to the core, it is necessary to reflect the beam of optical radiation back out after traversing the sample under study during the irradiation (see Fig. 2). Because of the effects of

nuclear irradiation on mirror materials and alignment problems associated with passing a beam of light down an 8-foot-long small-diameter port, the specimen configuration employed was a corner cube prism having a 1 1/2 in. usable diameter and a total optical path length of 6.2 cm, see Fig. 3. In this manner a great degree of misalignment can be tolerated before materially affecting the detected signal. This was determined in preliminary bench tests by closely approximating the final design of the instrument with regard to the physical relationship of the corner cube prism, optical path lengths and monochromator entrance slit dimensions. The results showed that the prism can be rotated $\pm 11^{o}$ about the optical axis before the intensity is decreased by a factor of two and that, further, no noticeable light variation results when the rotation angle was less than $\pm 3^{o}$. As a comparison, a misalignment on the order of minutes could not be tolerated if the specimen configuration was cylindrical and a flat mirror was used to reflect the beam back out of the reactor.

EXPERIMENTAL PROGRAM

Test Procedure

The experimental program was designed to accomplish three objectives:

1. To test for absorption due to free electrons produced during the irradiation process, which would be most apparent at infrared wavelengths.

2. To measure the absorption at the centers of the irradiation-induced absorption bands at 0.215 microns and 0.62 microns during and after an irradiation pulse and at a range of temperatures (ambient to 900°C).

3. To test for the existence of transient absorption, that is, absorption which is present only during the irradiation pulse.

The University of Illinois TRIGA Mark II reactor was operated in the pulse mode to utilize the high peak powers (on the order of 500 Megawatts) attainable in this mode of operation. Pulses at this power level supply peak neutron and gamma fluxes of approximately 5.4×10^{15} n/cm^2-sec and 6.1×10^{7} R/sec respectively with a pulse width at half peak power of thirty milliseconds. The neutron flux spectrum for pulses of this power is given in Table I. Figure 4 illustrates the neutron and gamma fluxes typically obtained from the TRIGA Reactor. Total integrated neutron and gamma doses provided by the reactor were of the order 2.3×10^{14} n/cm^2 and 2.6×10^{6} R respectively.

Table II summarizes the test conditions associated with each experiment. Five specimens were exposed to a total of 50 irradiation pulses. In addition, five bypass runs were made in which the light beam did not enter the reactor or traverse the specimen located therein. These runs were necessary to determine the effects of the reactor pulse upon the instrumentation and to obtain a correction factor to apply to the data runs. Forty-two irradiation pulses were made to measure the specimen transmission at an optical wavelength of 0.215 microns; six runs were made at wavelengths between 1.0 and 1.1 microns; and two runs were made at 0.62 microns. Two of the specimens, SC62-4 and SC62-5,* were given irradiation pulses while at elevated temperatures (between 300°C and 900°C) to examine the transient effects of the reactor pulse on the specimen absorption.

---

* The code used to refer to the specimens is the same as has been used in preceding work except that the first number refers to the path length of light through the specimens rather than specimen thickness (that is, the light travels 62 mm total distance in traversing the corner cube specimen).

Data was recorded on the Visicorder which plotted the signal level generated by the photomultiplier (detector output) as a function of time immediately before, during, and up to 1 second after the reactor pulse. In addition to monitoring the detector output, the Visicorder also recorded the peak portion of the reactor pulse and the output of a reference time mark generator for correlation purposes.

Source currents and detector voltages were monitored prior to each pulse and the conditions are summarized in Table II. As noted in this table, the hydrogen discharge lamp was unstable during the D-1 through D-11 pulses. This was corrected during the subsequent series by providing additional air cooling to the lamp itself.

In addition, for runs D-1 through D-11 and E-1 through E-16, the transmission of a standard specimen mounted external to the reactor was recorded immediately before each pulse to maintain a check on the stability and reliability of the transmittance measuring system.

Factors Affecting Transmission Data

Several factors were encountered during the test program which led to problems in interpreting the data. The most important of these was an apparent increase in the transmission of the specimens during the irradiation pulse, especially at elevated temperatures. Some of this apparent increase is directly attributable to the influence of the irradiation pulse itself upon the optical and electronic recording systems when operating the system in the ultraviolet at 0.215 microns. Figure 5 shows this radiation influence upon the instrumentation system for three bypass runs, that is, runs in which the optical radiation bypassed the reactor beam port in which the specimen was mounted. The radiation therefore went directly from the source chamber to the monochromator subsystem. Curve C-11 in Fig. 5 shows that the signal level using the original configuration increased some 19% during the peak of the pulse. Modifications were made in an effort to reduce this increase in signal level during the pulse. Since gamma irradiation can interact with photomultiplier tubes causing an effective increase in gain, two inches of lead shielding was placed around the 1P28 photomultiplier (curve D-13). No improvement resulted, although in this case the hydrogen discharge lamp was unstable (throughout runs D-1 through D-13). The light source chamber-cover was removed for the next set of runs to provide more efficient cooling of the lamp in an attempt to increase its stability. Curve E-11 illustrates the improvement obtained. Although not completely removed, the increase in signal level due to the reactor pulse is less than 7% which corresponds to an effective decrease in absorption of 0.011 cm^{-1} when applied to specimens with 6.2 cm path length. Unfortunately, bypass runs could not be made simultaneously with specimen runs because of the single-beam method of operation and therefore the bypass corrections applied to the data must be assumed as approximate corrections. The corrections were made as shown in Figs. 6 through 9.

Figure 6 illustrates a typical correction as applied to Run B-1 using the C-11 bypass run. It was assumed that the reactor pulse did not affect the gain of any component in the recording system but did add a noise signal to the true signal permitting a direct subtraction to obtain the correction. The change in the increase during the bypass run (C-11) was therefore subtracted from the specimen run (B-1) to obtain the corrected signal. No corrections were necessary before and after the pulse and therefore the data points of specimen run and corrected run agree.

Bypass data used to correct the elevated temperature runs are shown in Figs. 7 through 9. Figure 7 shows the bypass signal (run E-11) and three specimen runs at elevated temperatures: run E-8 at 300°C, run E-1 at 500°C and run E-5 at 900°C. Figure 8 illustrates the typical signal levels after subtracting the change in the signal level which occurred during the bypass run. In Fig. 9 the signal levels have been converted to transmittance values by comparing the signal levels to the standard specimen signal levels which were obtained prior to each run. Since a single-beam technique was employed, long term measurements (greater than a second) are subject to inaccuracies due to long term drift of the light source, photomultiplier and associated electronics. This is not critical during a single pulse since the transmittance change during a single pulse can be compared to the immediate pre-pulse transmittance (70 milliseconds before the peak of the pulse) to obtain the change in transmissivity and absorption during and immediately after a particular pulse. A standard specimen was inserted into the optical beam prior to the pulse during runs D and E to measure and reduce the effect of drift on the long-term measurements. Since the standard specimen could not be mounted in identically the same position as the specimens, this measurement was incorporated into the data to account for the relative changes of specimen transmission between the pulses and not as an absolute value of the transmittance. For example, the infrared and red spectral runs show that the specimen transmits more signal than the standard, as much as 2.15 times. Since these spectral runs were made with a narrower slit width (0.171 mm as opposed to 0.40 mm in the ultraviolet) and since the position of the 45° prism was maximized for the test specimen and not the standard, it is possible that the standard specimen deviated the beam slightly so as not to intercept the entrance slit of the monochromator in the same way as the test specimens.

Ambient Temperature Studies at 0.215 Microns

Two specimens, SC62-2 and SC62-3, were run in the ultraviolet at 0.215 microns at ambient temperature. The test conditions and post irradiation heating schedule are summarized in Table II. Each specimen was separately exposed to a total of 10 pulses consisting of two series of five pulses each. Between the two series, the specimens were removed from the reactor and heat treated in a small furnace. Specimen SC62-2 was heated at 508°C for 15 minutes whereas specimen SC62-3 was heated at 862°C for 30 minutes.

The total accumulated absorption coefficient after each step for specimen SC62-2 is shown in Fig. 10. Although some ambient temperature bleaching occurs between the pulses, this bleaching is incomplete in the twenty minute interim period. Also indicated in Fig. 10 is the incomplete defect annealing by the heat treatment at 508°C. Series 6 through 10 shows that a more rapid growth of absorption occurs during pulses B-6 and B-7 than for B-1 and B-2. This is interpreted as filling defects created during the first series which were not annealed during the heat treatment.

The total accumulated absorption coefficient after each step for specimen SC62-3 is shown in Fig. 11. The data is similar to that for SC62-2 in Fig. 10 with one exception. The heat treatment of 862°C for 30 minutes apparently annealed the defects produced during pulses C-1 through C-5 more completely since the growth of color in pulses C-6 through C-10 is nearly identical to the preceding five pulses.

Figures 12 through 15 illustrate the single pulse data obtained with each ambient temperature specimen. For specimen SC62-2, pulses B-1 through B-5 are shown in Fig. 12 and pulses B-6 through B-10, after the heat treatment, in Fig. 13. Figures 14 and 15 show similar data for specimen SC62-3. In each case the transmissivity before, during and immediately after the reactor pulse is plotted. The transmissivity is obtained by comparing the signal level during the pulse to the signal level immediately before the pulse (at time equal to -70 milliseconds). The curves therefore show the reduction in transmissivity induced by the reactor pulse. Succeeding pulses produce incrementally more absorption indicating again that only partial room-temperature bleaching of the irradiation-induced defects is occurring between pulses which are colored in succeeding pulses.

Elevated Temperature Studies at 0.215 Microns

Twenty-two test runs were made at 0.215 microns over a range of specimen temperatures from 300°C to 900°C using two samples, SC62-4 and SC62-5. The test conditions associated with these runs (Series D and E) are given in Table II. Figures 16 and 17 illustrate the pre-pulse and post-pulse (200 milliseconds after the pulse peak) absorption coefficient of these two specimens. The data are plotted as a function of pulse number for each series indicating the temperature history during the pulsing sequence. The data, as plotted, include the absorption due to temperature, that is, the values plotted are the sum of the irradiation-induced absorption coefficient and the increase in absorption due to the normal temperature shift of the ultraviolet cutoff in fused silica (see Ref. 1). The pre-pulse absorption coefficients are plotted in Fig. 18 to illustrate the familiar increase in absorption with temperature as a relatively smooth variation. These values are higher than those obtained in Ref. 1 but probably include temperature dependent experimental factors, especially the large specimen-to-monochromator distance. As previously mentioned, the increase in absorption coefficient with each

successive pulse at ambient temperature is attributed to the failure to bleach radiation-induced damage at ambient temperature and thus represents a build-up or growth of damage. It would appear from Figs. 16 and 17 that complete recovery did not occur after all the pulses at high temperature. This, however, is attributed to scatter in the data. This scatter for run series D is somewhat greater than for run series E and is believed to be due to the unsteadiness in the light source which accompanied run series D. Complete thermal recovery of the damage appears to occur in every case.

The single-pulse data for these series is plotted in Figs. 19 through 32. Again the signal during the pulse is compared to that before the pulse to obtain the true transmissivity during and after the reactor pulse. Two sets of figures are used for each specimen temperature. One set covers the time range from 70 milliseconds before to 160 milliseconds after the peak of the pulse to examine the transmissivity during the pulse. The other set condenses the time scale from 100 to 1000 milliseconds after the peak of the pulse to examine the bleaching of the irradiation-induced color. Especially for run series D, the bypass correction was too small to correct for all the signal level increase which occurred during the peak of the pulse. A portion of this effect may be attributed to the unsteadiness of the hydrogen discharge lamp during these runs.

All the curves show additional absorption being produced in the sample some 140 to 150 milliseconds after the peak of the pulse even though no absorption may have been present during the pulse. Initially, this was considered to be an experimental problem associated with gamma heating of the specimen and unequal cooling causing a schlieren-like effect to deviate the light beam, thus moving it off the slit and causing an apparent decrease in light intensity. Subsequent calculations indicated that (1) gamma heating would produce less than a 5°C temperature rise, and (2) the sample would require on the order of a minute to return to its original temperature. However, as seen in the curves, this absorption shows a relatively fast decay constant, and consequently cannot be attributed to gamma heating. It may be caused by a temperature dependent secondary radiation, e.g. fluorescence, or have some inherent time delay (half-life) for creation, but at present it is not understood.

Figure 33 shows a comparison of typical data obtained at various temperatures at times up to one second after the pulse. The first pulse in each temperature series has been selected to remove any ambiguities due to incomplete bleaching (especially in the cases of ambient and 300°C runs). It can be seen that the absorption at 150 milliseconds is greatest at 900°C and nearly equal at 500°C and 300°C. This absorption is, however, removed more rapidly at elevated temperatures: at 900°C the sample has returned to its pre-pulse value in less than one second; at 500°C, 75% recovery of the damage was observed after one second; and at 300°C, 60% recovery of the damage was observed after one second.

It is now of interest to estimate the equilibrium absorption in a fused silica specimen if the specimen were subjected to a continuous flux equal to the peak flux

in the TRIGA reactor. During such equilibrium operation, the rate of creation of absorption is given by the following equation:

$$d\alpha = k\phi_n \, dt \tag{1}$$

If no other processes are important, this can be integrated to give

$$\alpha = k\phi_n \, t \tag{2}$$

If the absorption is assumed to be bleached by a first-order kinetic process,

$$\frac{d\alpha}{\alpha} = - \frac{dt}{\theta} \tag{3}$$

At times greater than approximately 50 milliseconds following the TRIGA pulse, where the rate of creation of absorption sites is negligible, the absorption will decay by a logarithmic process which can be obtained by integration of Eq. (3).

$$\alpha = \alpha_o \, e^{-t/\theta} \tag{4}$$

For small values of absorption coefficient, the absorptivity is proportional to absorption coefficient. Therefore,

$$(1 - r) = (1 - r)_o \, e^{-t/\theta} \tag{5}$$

Values of reference absorptivity $(1 - r)_o$ were determined by the constructions illustrated in Figs. 34 through 40 and are summarized in Fig. 41. The time constants determined from the data shown in these figures are shown as a function of specimen temperature in Fig. 42. The line drawn through the data points has been weighted with the series E data since it is believed to be more reliable. Note that these decay time constants are approximately two orders of magnitude less than those indicated by the post-reactor decay time constants reported in Ref. 2.

By analogy with Eqs. (4) and (5), Eq. (2) can be approximated as

$$(1 - r)_o = k\phi_n \, t_o \tag{6}$$

or

$$k\phi_n = \frac{(1 - r)_o}{t_o} \tag{7}$$

The quantity t_o in Eqs. (6) and (7) represents the value of time equal to the total dose divided by the peak flux. This quantity for the TRIGA reactor pulses employed in the present test program is equal to approximately 2.3×10^{14} neutrons/cm^2 divided by 5.3×10^{15} neutrons/cm^2-sec, or 0.043 sec.

The equilibrium absorption coefficient, α_e, for long exposure times can be obtained by equating the expression for the rate of creation of absorption in Eq. (1) to the negative value of the expression for the rate of annealing of absorption in Eq. (3). Therefore,

$$\alpha_e \frac{dt}{\theta} = k\phi_n \, dt \tag{8}$$

or

$$\alpha_e = k\phi_n \theta \tag{9}$$

Substituting from Eq. (2) yields

$$\alpha_e = \theta \alpha_o / t_o \tag{10}$$

Plotted as a function of temperature in Fig. 43 are values of equilibrium absorption coefficient as calculated from the data in Figs. 41 and 42 and a value of t_o of 0.043 sec. These values apply for a continuous flux equal to the peak TRIGA flux of 5.3×10^{15} n/cm^2-sec. At 900°C the equilibrium absorption coefficient is estimated to be approximately 0.7 cm^{-1}. The peak TRIGA fast neutron flux is approximately half of the flux in a 4600 Megawatt nuclear light bulb reactor according to the studies of Ref. 4. The resulting indicated equilibrium absorption coefficient of 1.4 cm^{-1} for the engine at the middle of an absorption band centered at a wavelength of 0.215 microns (twice that calculated for the peak TRIGA flux) should have little adverse effect on a nuclear light bulb reactor. However, the calculated equilibrium absorption coefficient would be two orders of magnitude higher if the decay times from the post-reactor tests of Ref. 2 were employed; this increased equilibrium absorption coefficient would have a substantial adverse effect on the characteristics of a nuclear light bulb reactor.

Studies at Visible and Near-Infrared Wavelengths

Eight runs were made at wavelengths other than 0.215 microns: six at 1.0 to 1.1 microns and two at 0.625 microns. The region at 0.625 microns is of interest because it is the center of an irradiation-induced absorption band as reported in Ref. 1. Figure 44 shows the transmissivity data obtained at 0.625 microns with specimen SC62-5 at ambient temperature and at 500°C. The ambient temperature run shows an almost immediate production of absorption whereas at 500°C the absorption peaks some 160 to 180 milliseconds after the pulse (similar to the ultraviolet high-temperature runs). The maximum absorption induced was 0.01 cm^{-1} and, in the case of the 500°C test, was entirely removed in less than 1 second.

The infrared region (1.0 to 1.1 microns)was monitored during six pulses to test for free electron absorption, since in high-gamma-flux fields sufficient free electrons could be produced to cause measurable absorption. In the data for specimen

SC62-1 (run Series A, Table II) no change in transmittance was observed for runs A-1 and A-2. Small changes were observed at 1.05 and 1.1 microns which were in the direction of increased signal, corresponding to a negative absorption coefficient of 0.015 cm^{-1}. Since a calibration bypass run was not made for this series, the data is not presented. However, Fig. 45 shows the results for run E-15 for which a bypass run was made. The transmissivity change is immeasurable indicating that no absorption due to free electrons was detected.

REFERENCES

1. Douglas, F. C. and R. M. Gagosz: Experimental Investigations of Thermal Annealing of Nuclear-Reactor-Induced Coloration in Fused Silica. United Aircraft Research Laboratories Report D-910082-7, March 1965. Also issued as NASA CR-304.

2. Douglas, F. C., R. Gagosz, and M. A. DeCrescente: Optical Absorption in Transparent Materials Following High Temperature Reactor Irradiation. United Aircraft Research Laboratories Report F-910485-2, September 1967. To be issued as NASA CR Report.

3. Edwards, O. J.: Optical Absorption Coefficients of Fused Silica in the Wavelength Range 0.17 to 3.5 Microns from Room Temperature to 980°C NASA TN D-3257 February 1966.

4. Latham, T. S.: Nuclear Criticality Studies of Specific Nuclear Light Bulb and Open Cycle Gaseous Nuclear Rocket Engines. United Aircraft Research Laboratories Report F-910375-2, September 1967. To be issued as NASA CR Report.

LIST OF SYMBOLS

k	Constant governing variation of absorption coefficient with neutron flux [see Eq. (2)], cm/neutron
t	Time, sec
t_o	Value of time determined by dividing total neutron dose by peak TRIGA neutron flux, sec
α	Absorption coefficient, cm^{-1}
α_o	Absorption at beginning of time interval, cm^{-1}
α_e	Calculated equilibrium absorption coefficient for continuous operation at peak TRIGA neutron flux, cm^{-1}.
θ	Time constant for decay of radiation-induced absorption [see Eq. (4)], sec
r	Transmissivity, I/I_o
ϕ_n	Neutron flux, neutron/cm^2-sec

TABLE I

Neutron Flux Spectrum for a Typical TRIGA Pulse

Energy Range	Neutron Flux 10^{15} n/cm^2-sec	% of Total Flux
Thermal	2.12	39.2
Epithermal	.55	10.3
1 Kev to 0.75 Mev	.86	16.0
0.75 to 1.50 Mev	1.05	19.5
1.50 to 2.90 Mev	.51	9.5
2.90 Mev to ∞	.29	5.5
Total	5.38	100.0

TABLE II

TRIGA In-Reactor Irradiation Test Conditions

Specimen	Run No.	Peak Neutron Flux, 10^{15} n/cm^2-sec	Neutron Dose, 10^{14} n/cm^2	Peak Gamma Flux, 10^7 R/sec	Gamma Dose, 10^8R	Wavelength, Microns	Specimen Temperature, Degrees Centigrade	Source Current, Amps	Photomultiplier, Voltage	Slit Width, Millimeters	Bypass Run Used to Correct Data
SC62-1	A-1	5.18	2.28	5.82	2.56	1.0	Ambient	18	1200	0.20	-
	2	5.25	2.30	5.90	2.58	1.0	"	"	"	"	-
	3	5.19	2.28	5.83	2.56	1.05	"	"	"	"	-
	4	5.25	2.38	5.90	2.68	1.1	"	"	"	"	-
	5	5.23	2.30	5.88	2.58	1.1	"	"	"	"	-
SC62-2	B-1	5.22	2.28	5.87	2.56	0.215	Ambient	0.300	700	0.40	C-11
	2	5.22	2.29	5.87	2.57	"	"	"	"	"	"
	3	5.31	2.30	5.99	2.58	"	"	"	"	"	"
	4	5.28	2.30	5.93	2.58	"	"	"	"	"	"
	5	5.29	2.30	5.94	2.58	"	"	"	"	"	"
	6 (a)	5.40	2.32	6.06	2.61	"	"	"	"	"	"
	7	5.34	2.31	5.99	2.60	"	"	"	"	"	"
	8	5.36	2.31	6.02	2.60	"	"	"	"	"	"
	9	5.34	2.31	5.99	2.60	"	"	"	"	"	"
	10	5.35	2.31	6.01	2.60	"	"	"	"	"	"
SC62-3	C-1	5.31	2.30	5.96	2.58	0.215	Ambient	0.300	700	0.40	C-11
	2	5.29	2.30	5.94	2.58	"	"	"	"	"	"
	3	5.31	2.30	5.96	2.58	"	"	"	"	"	"
	4	5.33	2.35	5.98	2.64	"	"	"	"	"	"
	5	5.34	2.31	5.99	2.60	"	"	"	"	"	"
	6 (b)	5.34	2.30	5.99	2.58	"	"	"	"	"	"
	7	5.34	2.30	5.99	2.58	"	"	"	"	"	"
	8	5.33	2.31	5.98	2.60	"	"	"	"	"	"
	9	5.35	2.31	6.01	2.60	"	"	"	"	"	"
	10	5.38	2.32	6.04	2.61	"	"	"	"	"	"
	11 (c)	5.40	2.33	6.06	2.62	"	"	"	"	0.20	-
SC62-4	D-1	5.46	2.31	6.13	2.60	0.215	700	0.300 (d)	700	0.40	D-13
	2	5.52	2.35	6.20	2.64	"	700	"	"	0.40	"
	3	5.53	2.28	6.21	2.56	"	700	"	"	0.40	"
	4	5.48	2.28	6.15	2.56	"	700	"	"	0.40	"
	5	5.46	2.26	6.13	2.54	"	800	"	"	0.40	"
	6	5.46	2.28	6.13	2.56	"	800	"	"	0.40	"
	7	5.45	2.29	6.12	2.57	"	900	"	"	0.40	"
	8	5.46	2.25	6.13	2.53	"	900	"	"	0.40	"
	9	5.46	2.32	6.13	2.61	"	600	"	"	0.40	"
	10	5.45	2.25	6.12	2.53	"	600	"	"	0.40	"
	11	5.45	2.24	6.12	2.52	"	600	"	"	0.40	"
	12	5.41	2.24	6.08	2.52	"	600	"	"	0.40	"
	13 (c)	5.43	2.24	6.10	2.52	"	--	"	"	0.18	-
SC62-5	E-1	5.40	2.24	6.06	2.52	0.215	500	0.300	700	0.40	E-11
	2	5.38	2.24	6.04	2.52	"	500	"	"	0.40	"
	3	5.36	2.24	6.02	2.52	"	500	"	"	0.40	"
	4	5.37	2.25	6.03	2.53	"	500	"	"	0.40	"
	5	5.40	2.24	6.06	2.52	"	900	"	"	0.40	"
	6	5.40	2.28	6.06	2.56	"	900	"	"	0.40	"
	7	5.34	2.25	5.99	2.53	"	900	"	"	0.40	"
	8	5.61	2.31	6.30	2.60	"	300	"	"	0.40	"
	9	5.46	2.25	6.13	2.53	"	300	"	"	0.40	"
	10	5.40	2.30	6.06	2.58	"	300	"	"	0.40	"
	11 (c)	5.38	2.28	6.04	2.56	"	-	"	"	0.185	-
	12	5.38	2.24	6.05	2.52	0.62	66	18	1200	0.171	E-13
	13 (c)	5.34	2.25	5.99	2.53	0.62	-	"	"	"	-
	14 (c)	5.34	2.24	5.99	2.52	1.0	-	"	"	"	-
	15	5.38	2.26	6.04	2.54	1.0	Ambient	"	"	"	E-14
	16	5.34	2.24	5.99	2.52	0.62	500	"	"	"	E-13

(a) Sample SC62-2 was annealed at 508°C for 15 minutes between pulses 5 and 6.
(b) Sample SC62-3 was annealed at 862°C for 30 minutes between pulses 5 and 6.
(c) Optical beam did not pass through specimen in reactor for bypass run.
(d) The hydrogen lamp was unstable during runs D-1 through D-11.

OPTICAL SCHEMATIC FOR IN-REACTOR TRANSMISSION MEASUREMENTS

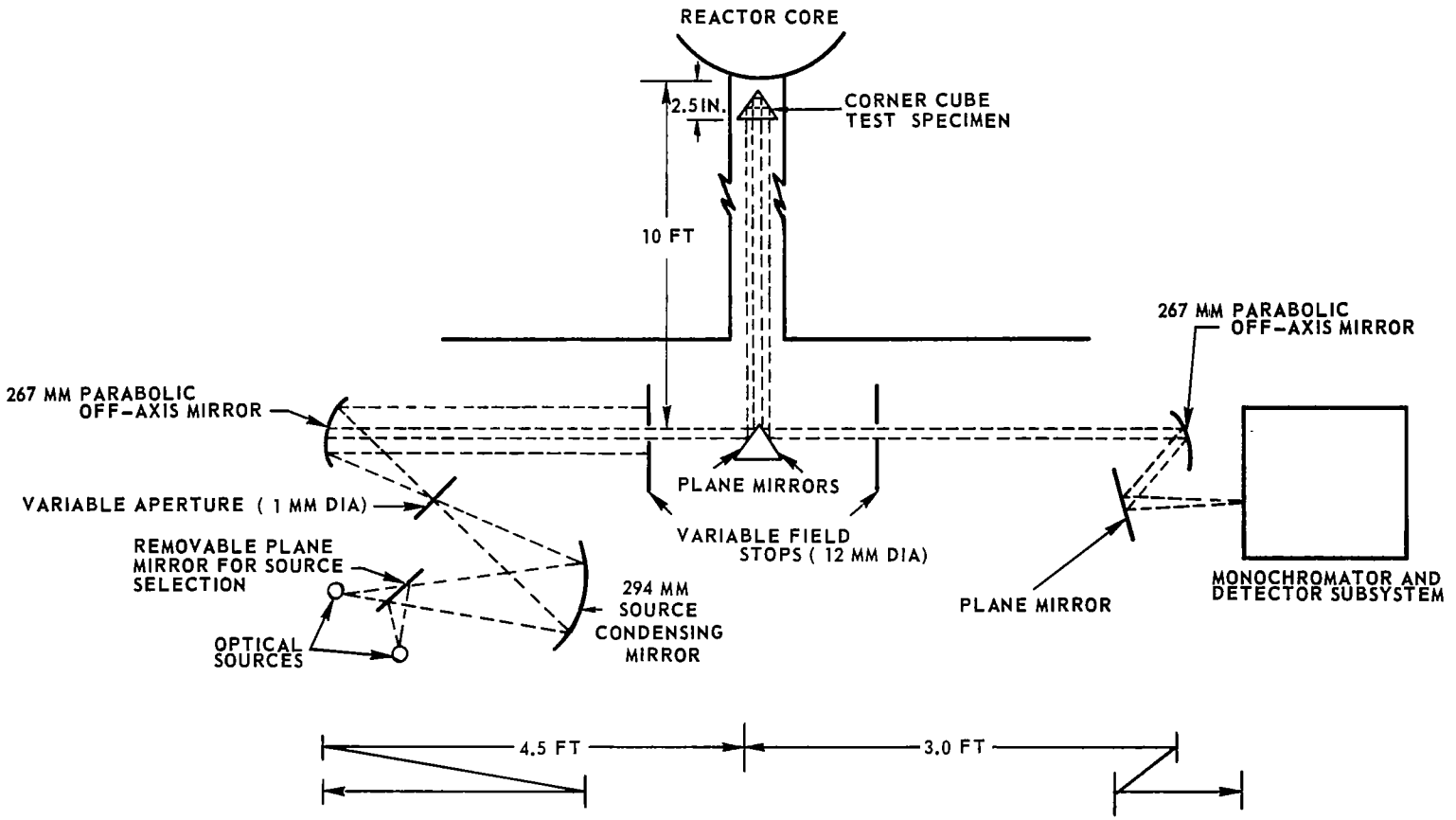

FIG. 1

LOCATION OF SPECIMEN AND INSTRUMENTATION RELATIVE TO TRIGA REACTOR CORE

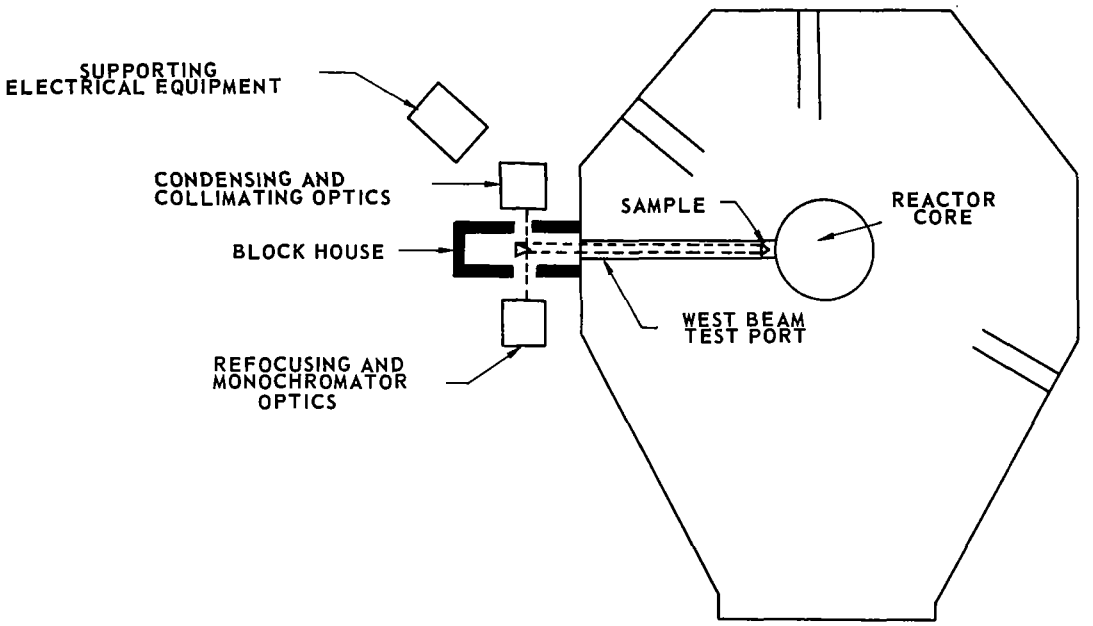

FIG. 2

FIG. 3

CORNER CUBE SPECIMEN

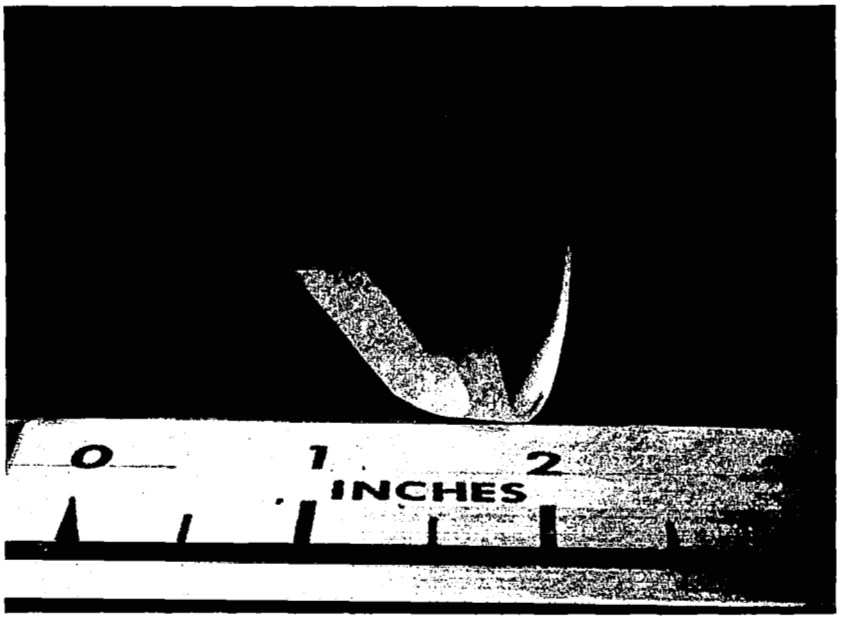

FIG. 4

TYPICAL NEUTRON AND GAMMA FLUX PROFILES OF TRIGA PULSE

RUN D–7

SYMBOL	FLUX
□	NEUTRON
○	GAMMA

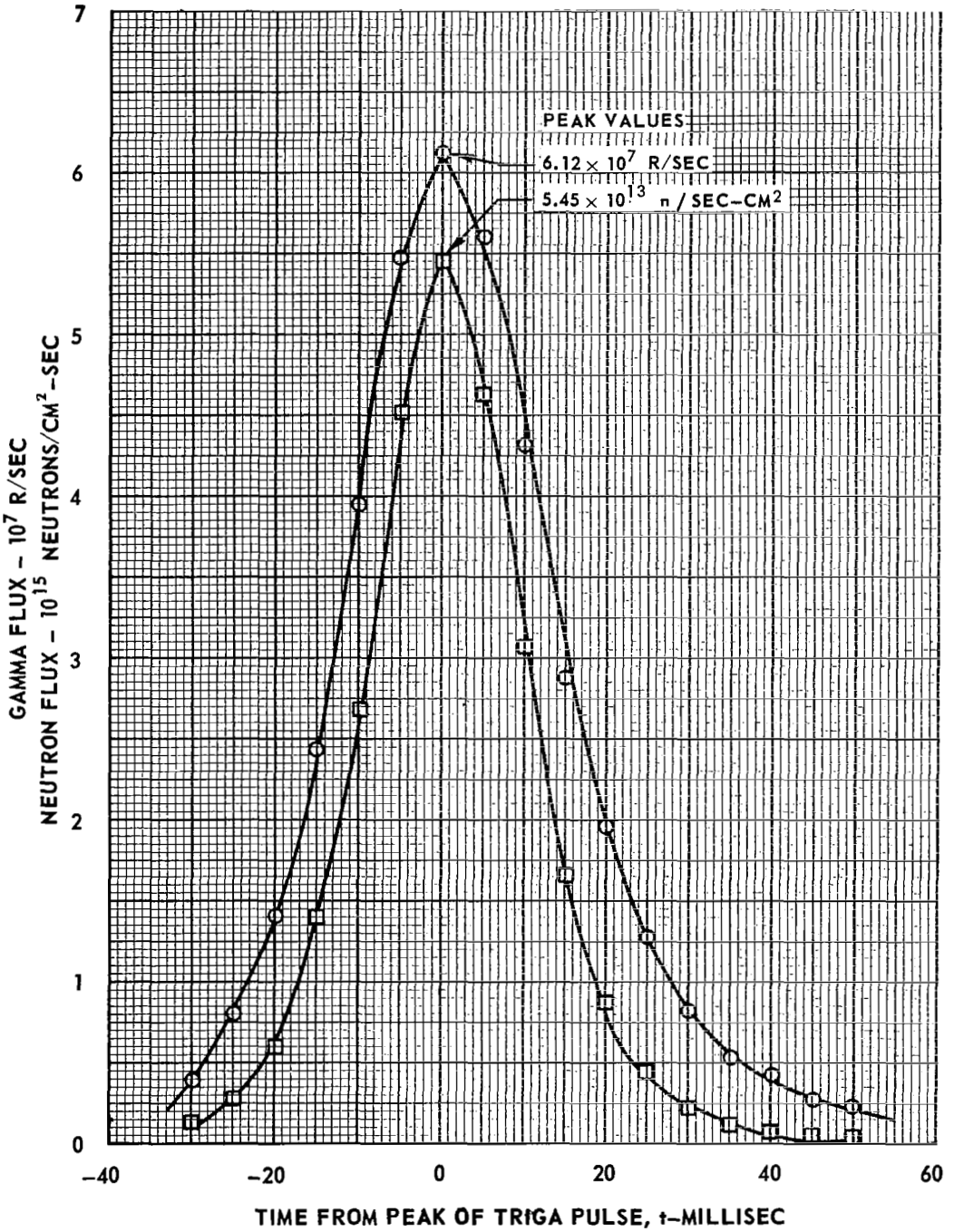

FIG. 5

COMPARISON OF RECORDED BYPASS SIGNAL LEVEL DURING TRIGA REACTOR PULSE

WAVELENGTH, λ = 0.215 MICRON

SYMBOL	RUN	NOTES
△	C-11	ORIGINAL CONFIGURATION
○	D-13	LEAD SHIELDING ADDED LIGHT SOURCE INTENSITY UNSTEADY
□	E-11	LIGHT SOURCE MADE STEADY WITH MORE EFFICIENT COOLING

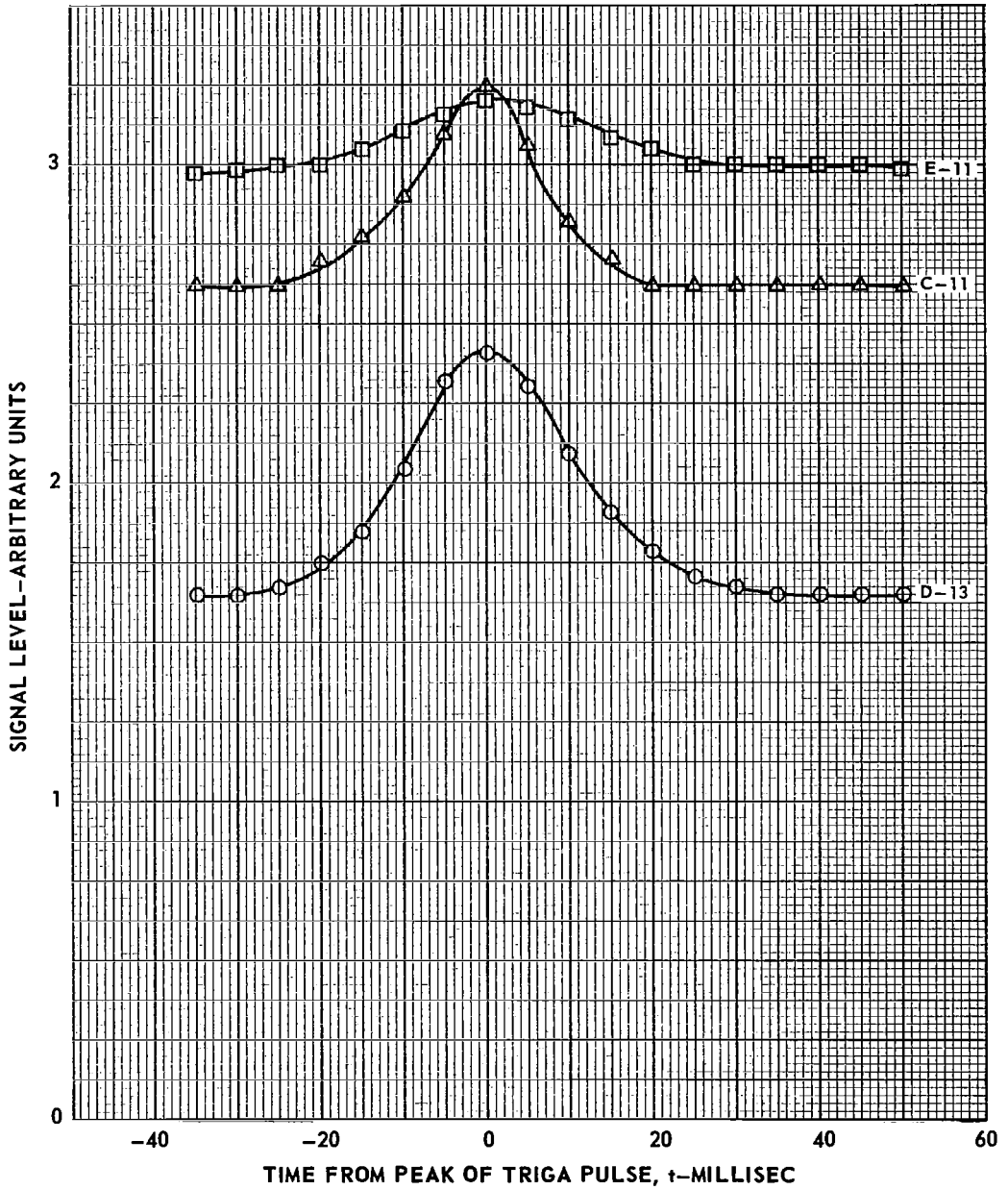

FIG. 6

TYPICAL DATA FOR AMBIENT SPECIMEN TEMPERATURE

SPECIMEN SC 62-2

WAVELENGTH, λ = 0.215 MICRON

SYMBOL	RUN	DESCRIPTION
○	B-1	SPECIMEN
□	C-11	BYPASS
△	-	CORRECTED

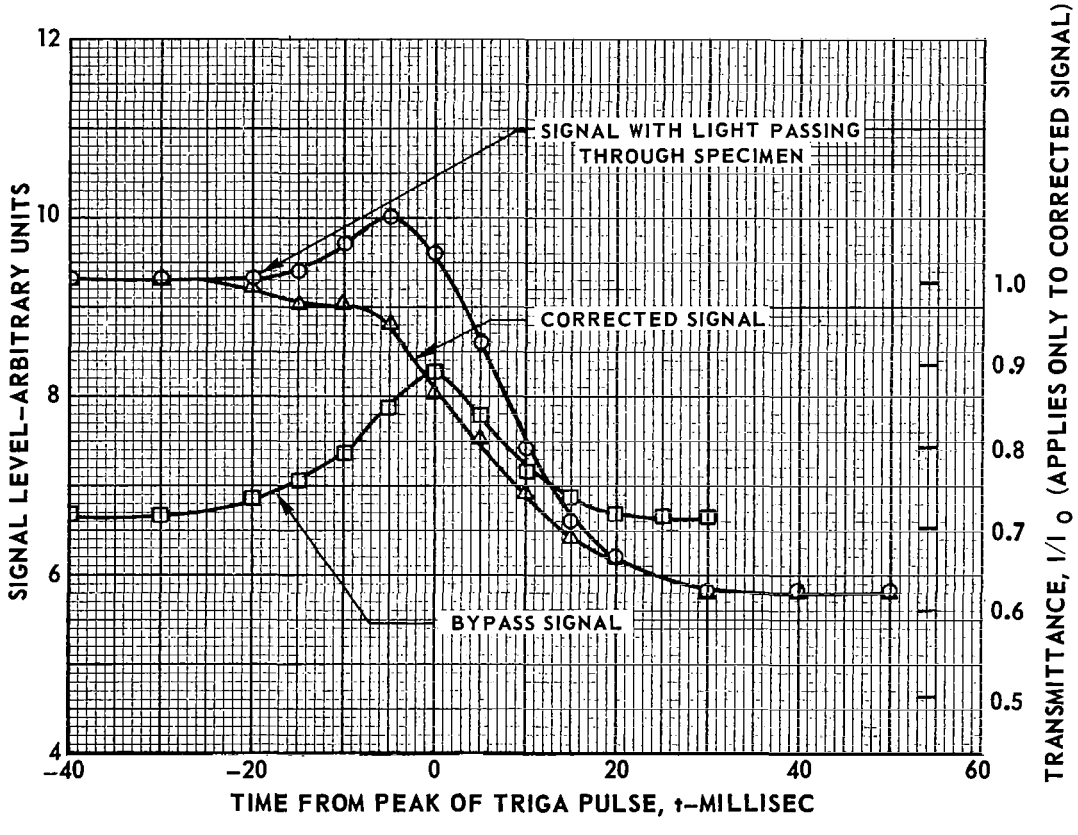

FIG. 7

TYPICAL RECORDED SIGNAL LEVELS FOR HIGH SPECIMEN TEMPERATURES

SPECIMEN SC 62–5

WAVELENGTH, λ = 0.215 MICRON

SYMBOL	RUN	TEMPERATURE
□	E–8	300 C
○	E–1	500 C
△	E–5	900 C
◇	E–11	BYPASS

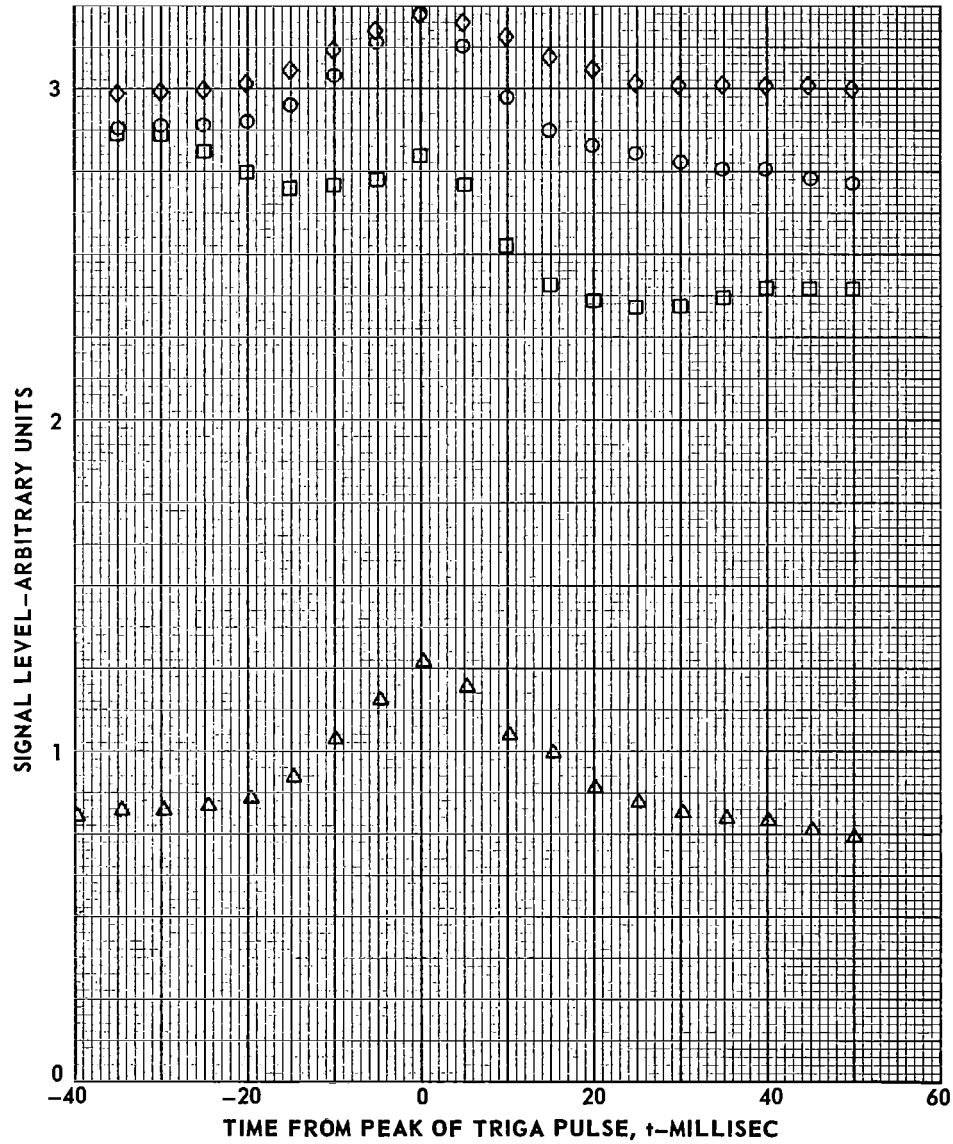

FIG. 8

TYPICAL SIGNAL LEVELS AFTER SUBTRACTING SIGNAL LEVEL OF BYPASS RUN FOR HIGH SPECIMEN TEMPERATURES

SPECIMEN SC 62–5

WAVELENGTH, λ= 0.215 MICRON

SYMBOL	RUN	TEMPERATURE
□	E–8	300 C
○	E–1	500 C
△	E–5	900 C

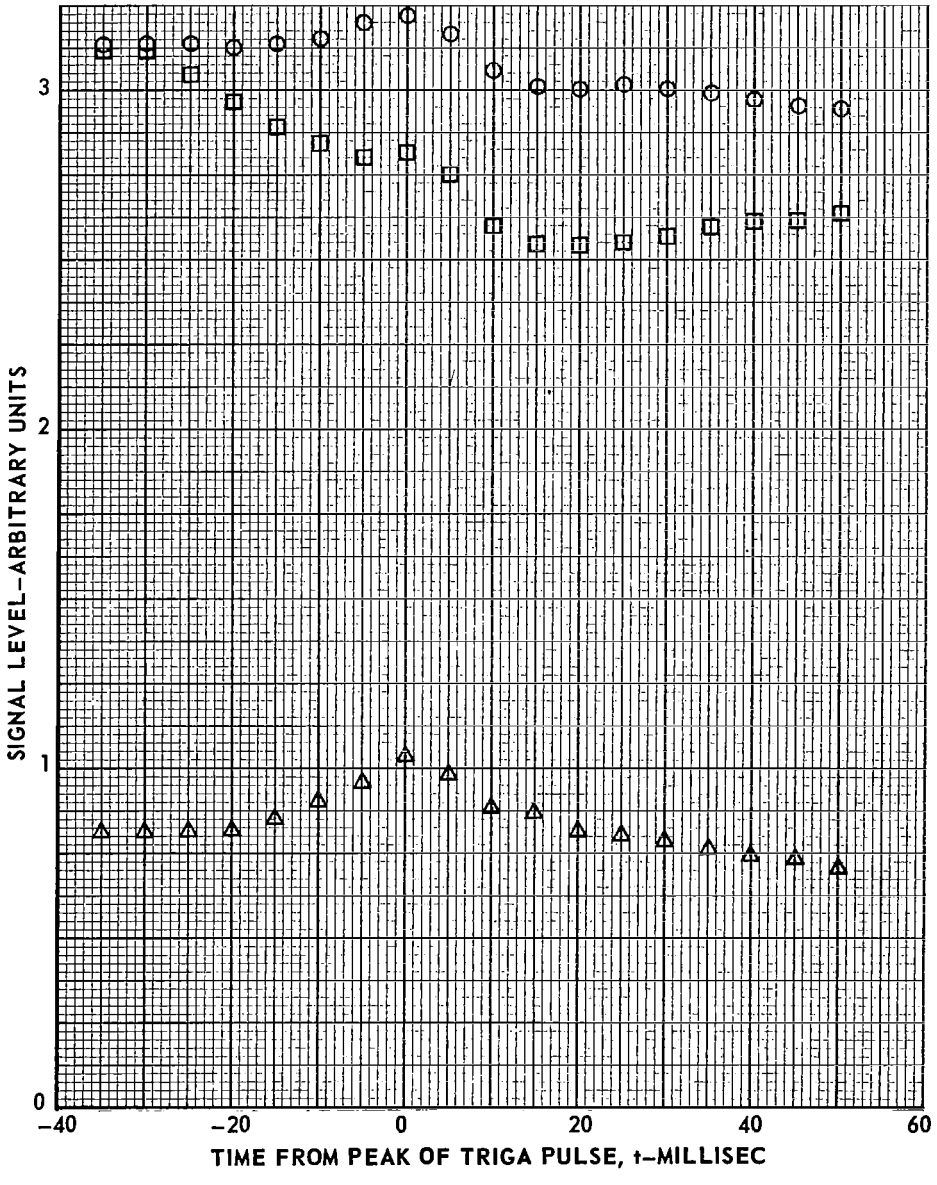

FIG. 9

TYPICAL TRANSMITTANCE FOR HIGH SPECIMEN TEMPERATURE

SPECIMEN SC 62–5

WAVELENGTH, $\lambda = 0.215$ MICRON

SYMBOL	RUN	TEMPERATURE
□	E–8	300 C
○	E–1	500 C
△	E–5	900 C

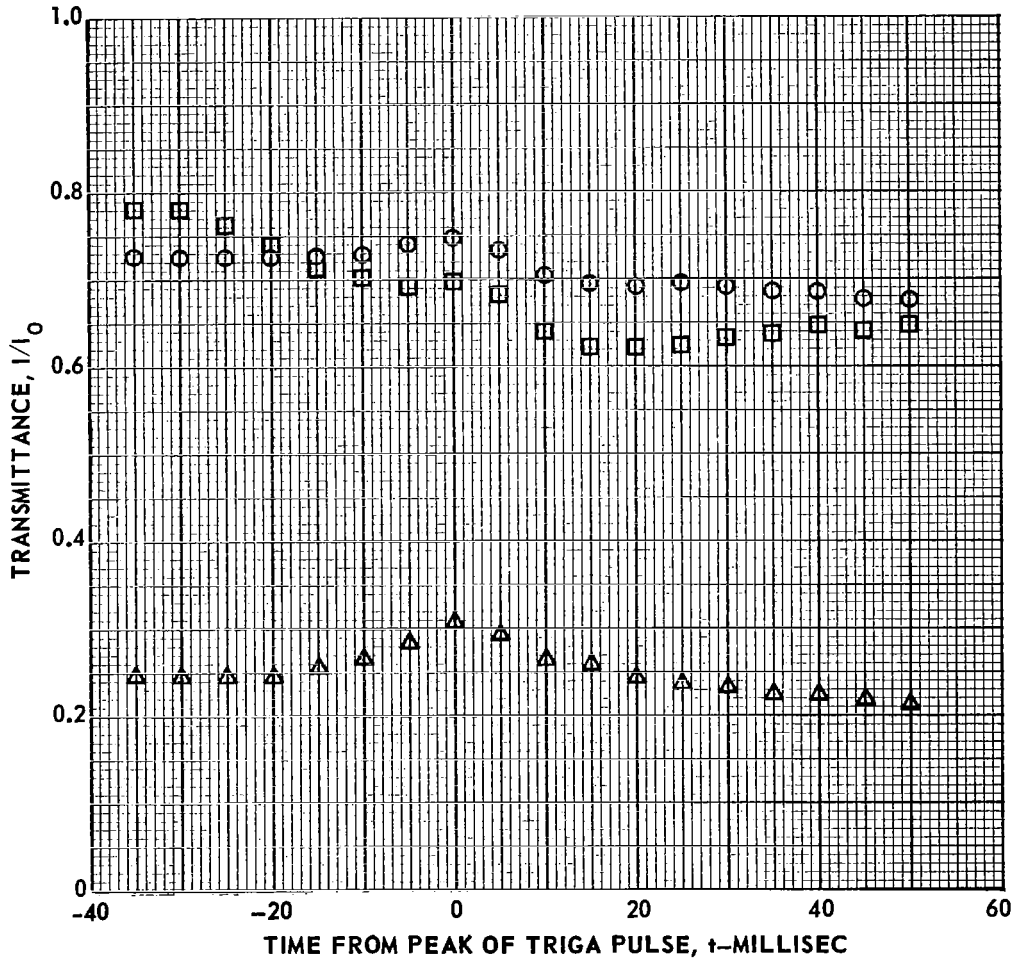

FIG. 10

ABSORPTION COEFFICIENTS MEASURED BEFORE AND AFTER SUCCESSIVE TRIGA PULSES FOR RUN SERIES B

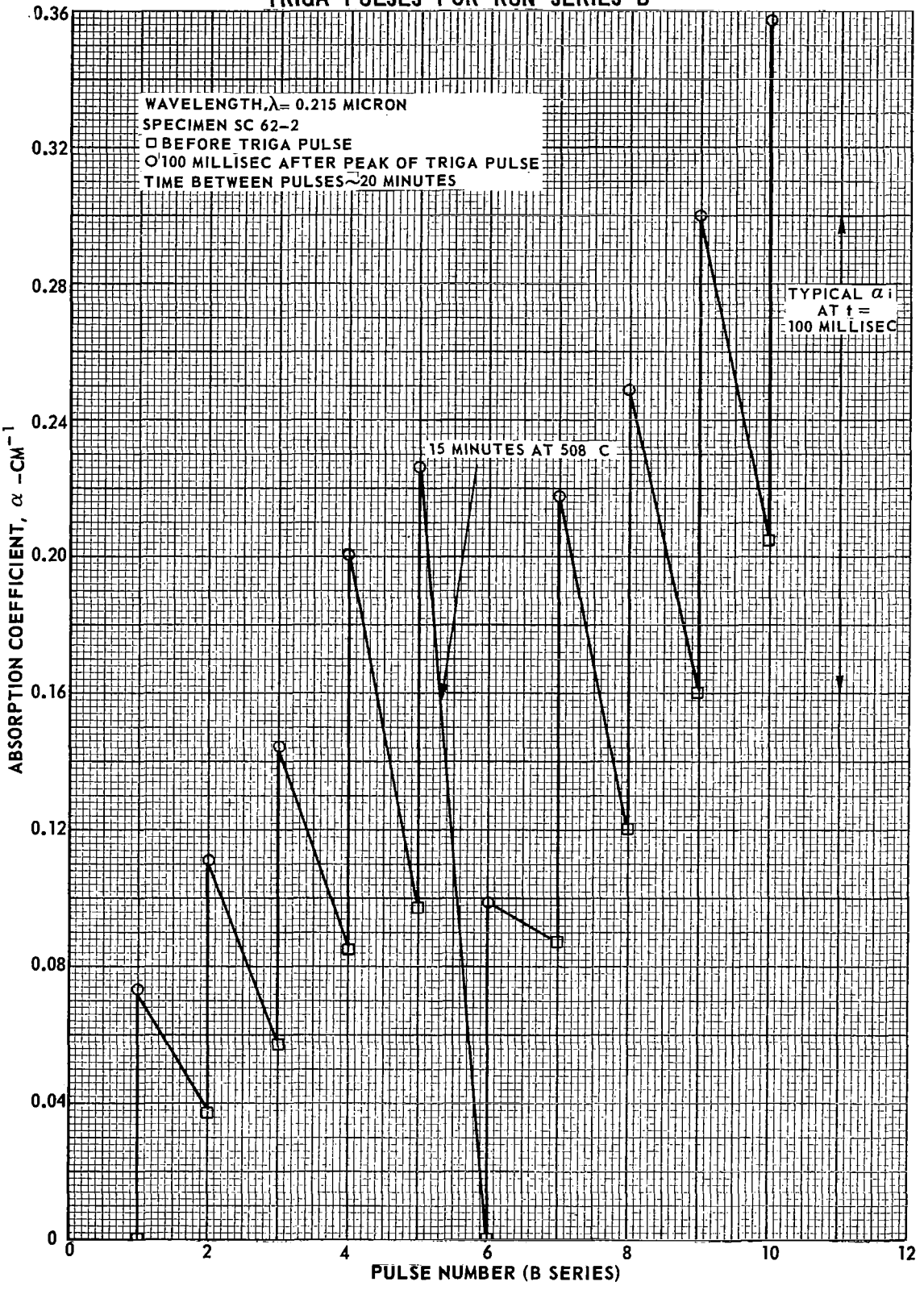

FIG. 11

ABSORPTION COEFFICIENTS MEASURED BEFORE AND AFTER SUCCESSIVE TRIGA PULSES FOR RUN SERIES C

SPECIMEN SC 62-3

WAVELENGTH, λ = 0.215 MICRON

□ BEFORE TRIGA PULSE
○ 100 MILLISEC AFTER PEAK OF TRIGA PULSE
TIME BETWEEN PULSES ~ 20 MINUTES

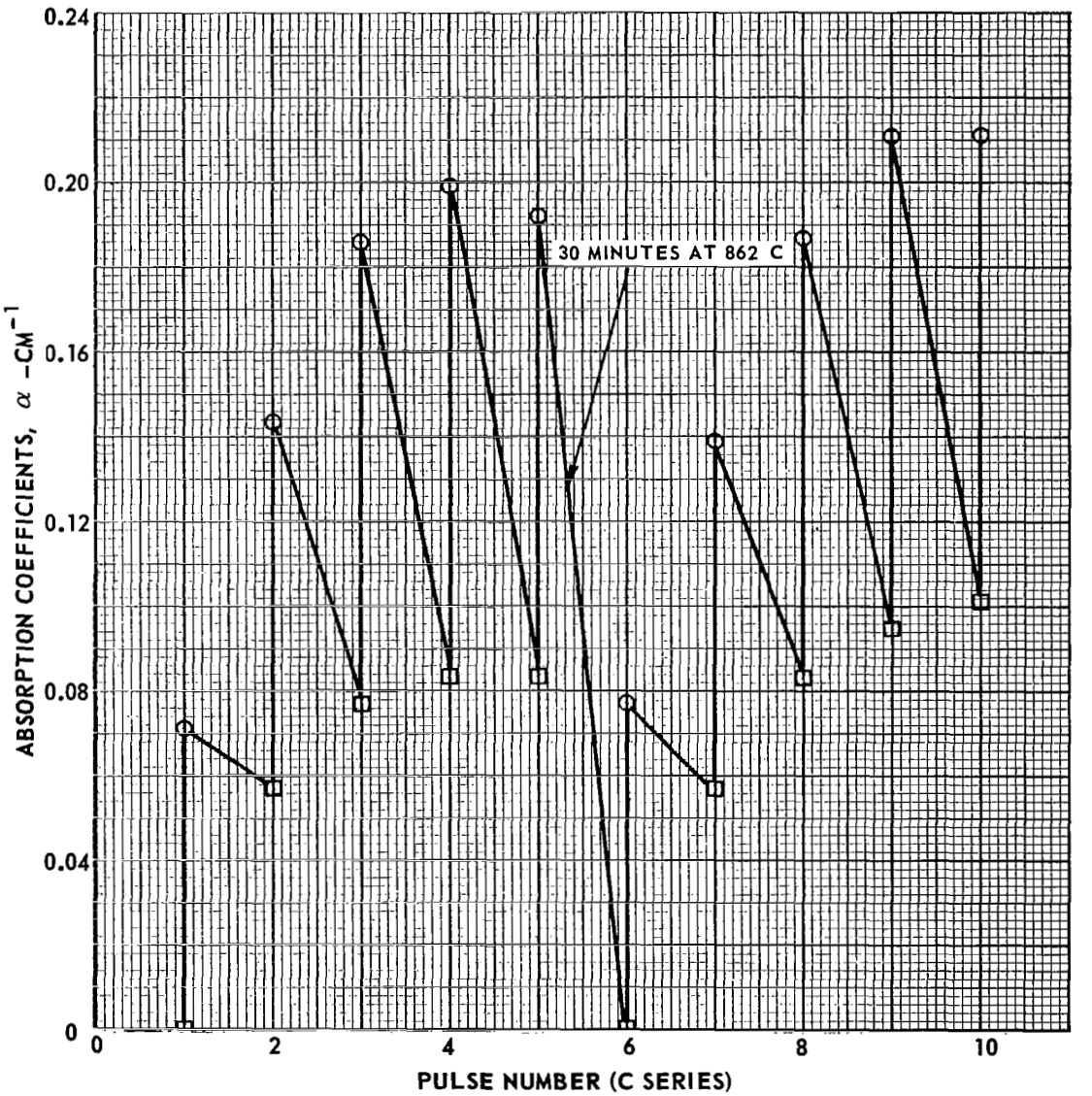

FIG. 12

TRANSMISSIVITY DURING RUNS B–1 THROUGH B–5 AT AMBIENT TEMPERATURE

SPECIMEN SC 62–2

WAVELENGTH, λ = 0.215 MICRON

SYMBOL	RUN	$(I/I_0)_{REF}$	FRACTIONAL BYPASS CORRECTION TO I/I_0 AT $t = 0$
○	B–1	1.0	0.172
△	B–2	0.796	0.216
□	B–3	0.699	0.246
◇	B–4	0.581	0.296
◿	B–5	0.538	0.320

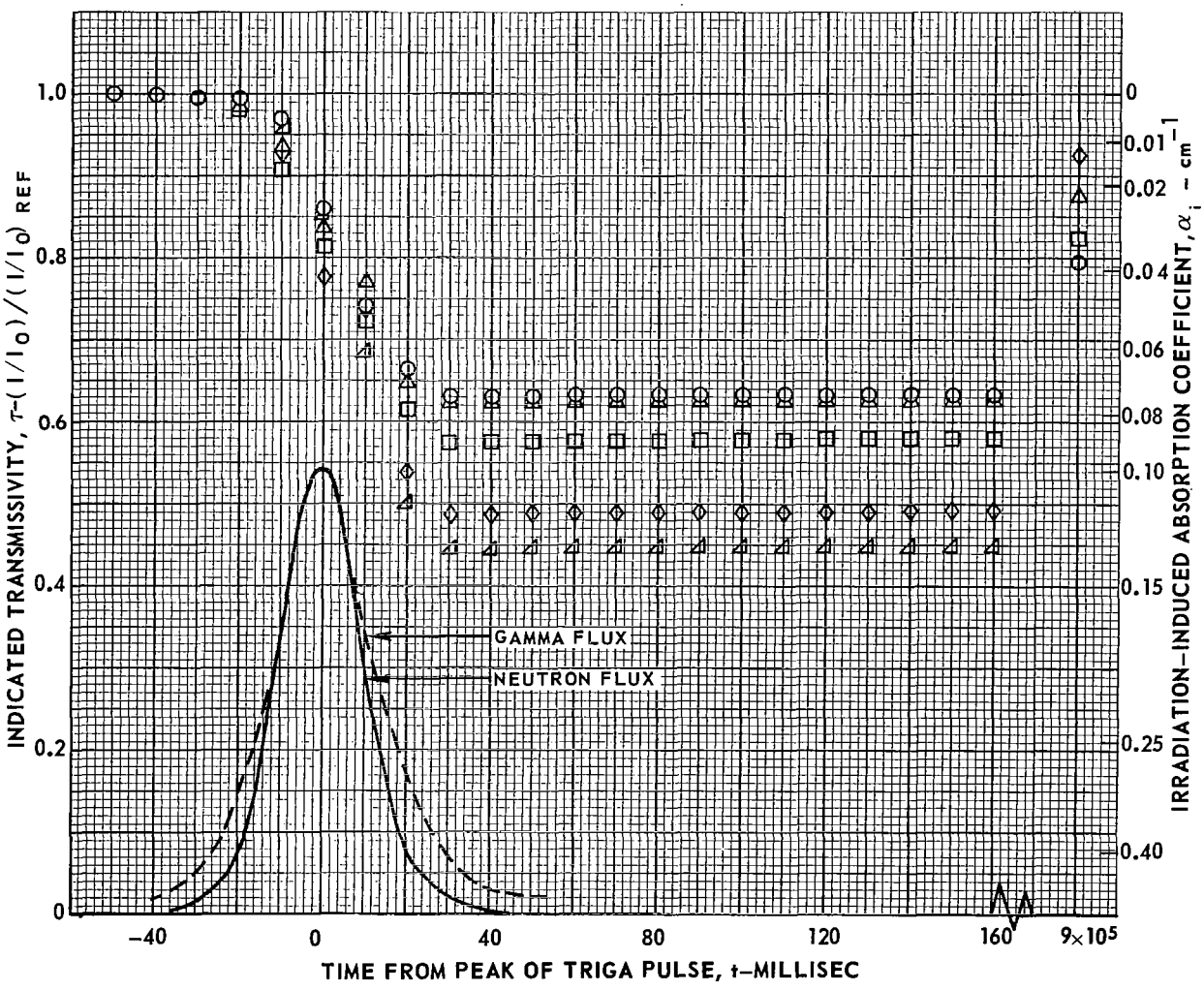

FIG. 13

TRANSMISSIVITY DURING RUNS B–6 THROUGH B–10 AT AMBIENT TEMPERATURE

SPECIMEN SC 62-2

WAVELENGTH λ = 0.215 MICRON

SYMBOL	RUN	$(I/I_0)_{REF}$	FRACTIONAL BYPASS CORRECTION TO I/I_0 AT $t=0$
○	B–6	1.00	0.182
△	B–7	0.568	0.320
□	B–8	0.466	0.391
◇	B–9	0.364	0.500
◿	B–10	0.272	0.67

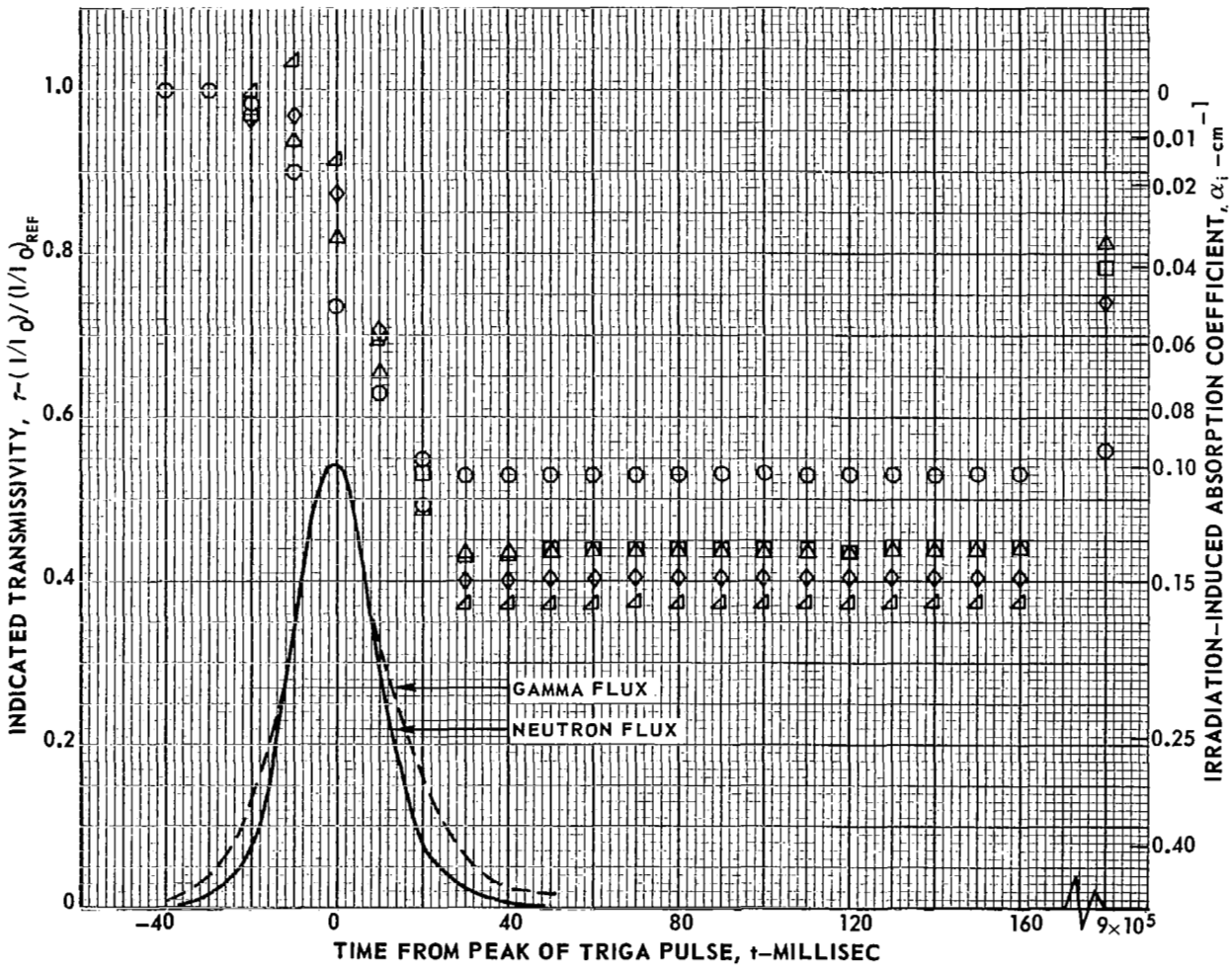

FIG. 14

TRANSMISSIVITY DURING RUNS C–1 THROUGH C–5 AT AMBIENT TEMPERATURE

SPECIMEN SC 62–3

WAVELENGTH, λ = 0.215 MICRON

SYMBOL	RUN	$(I/I_0)_{REF}$	FRACTIONAL BYPASS CORRECTION TO I/I_0 AT t=0
○	C–1	1.0	0.188
△	C–2	0.692	0.271
□	C–3	0.619	0.307
◇	C–4	0.588	0.320
⊿	C–5	0.588	0.320

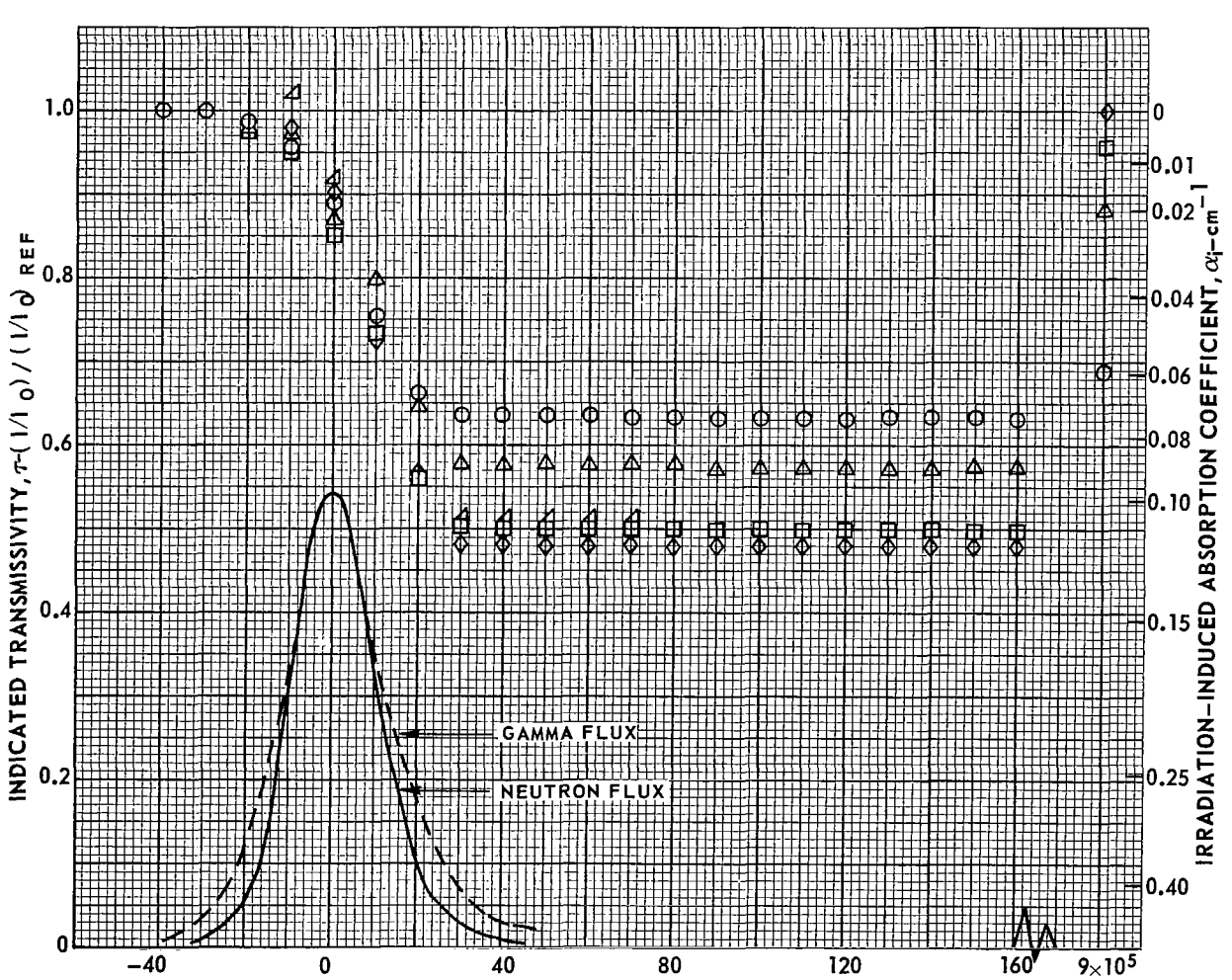

FIG. 15

TRANSMISSIVITY DURING RUNS C-6 THROUGH C-10 AT AMBIENT TEMPERATURE

SPECIMEN SC 62-3

WAVELENGTH, λ = 0.215 MICRON

SYMBOL	RUN	$(I/I_0)_{REF}$	FRACTIONAL BYPASS CORRECTION TO I/I_0 AT t=0
○	C-6	1.0	0.174
△	C-7	0.696	0.250
□	C-8	0.588	0.296
◇	C-9	0.544	0.320
◿	C-10	0.522	0.334

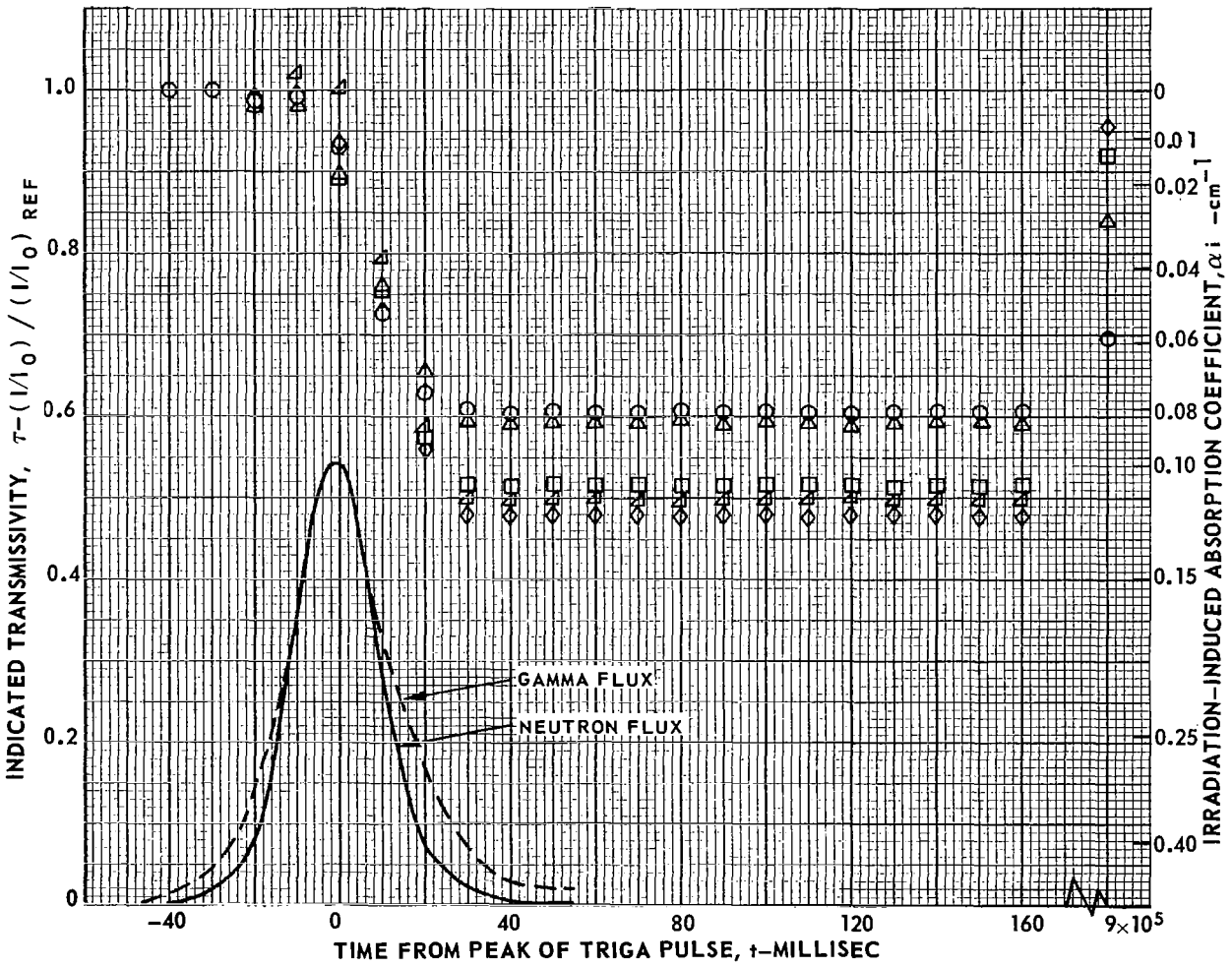

FIG. 16

ABSORPTION COEFFICIENTS MEASURED BEFORE AND AFTER SUCCESSIVE TRIGA PULSES FOR RUN SERIES D

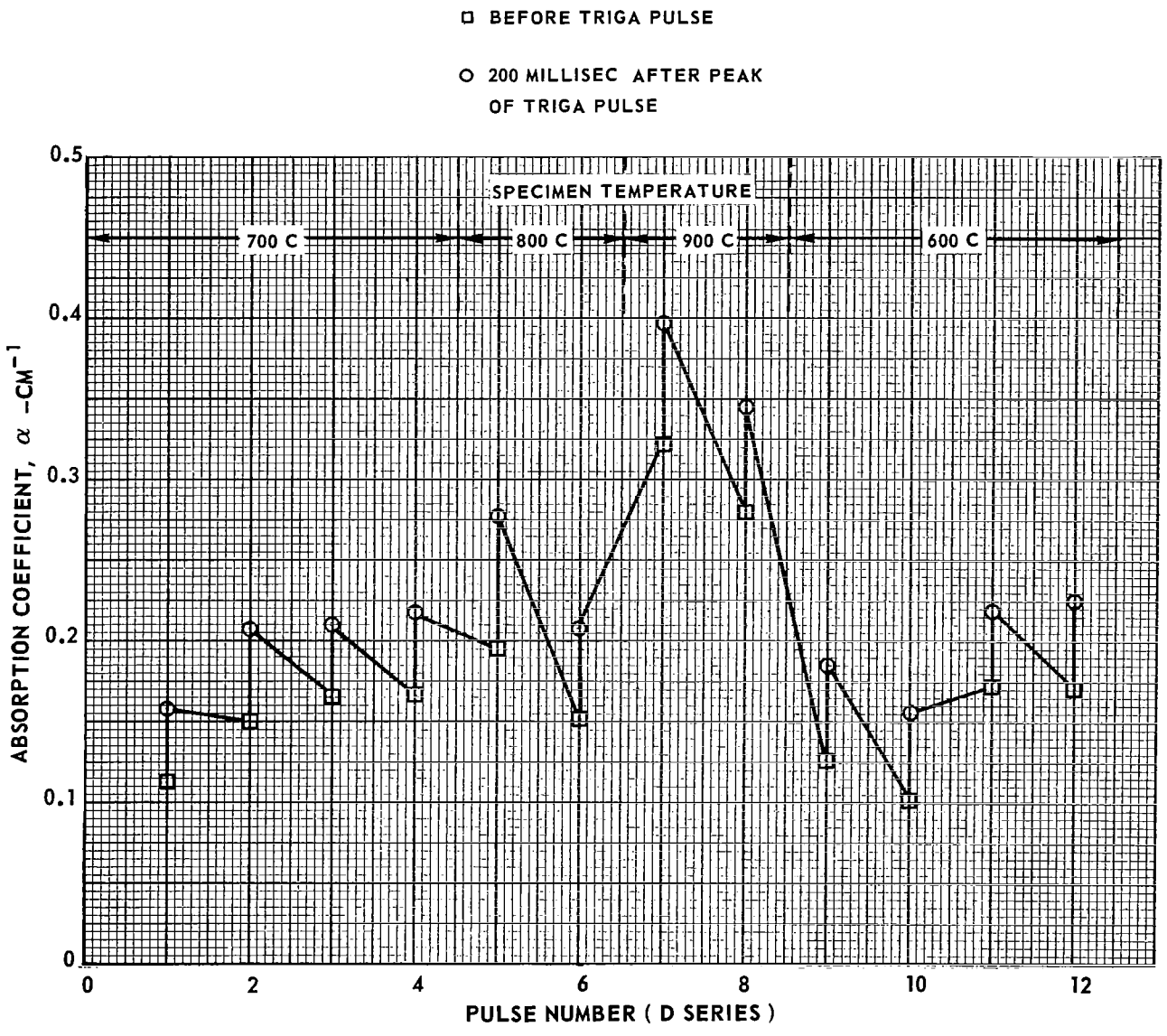

FIG. 17

ABSORPTION COEFFICIENTS MEASURED BEFORE AND AFTER SUCCESSIVE TRIGA PULSES FOR RUN SERIES E

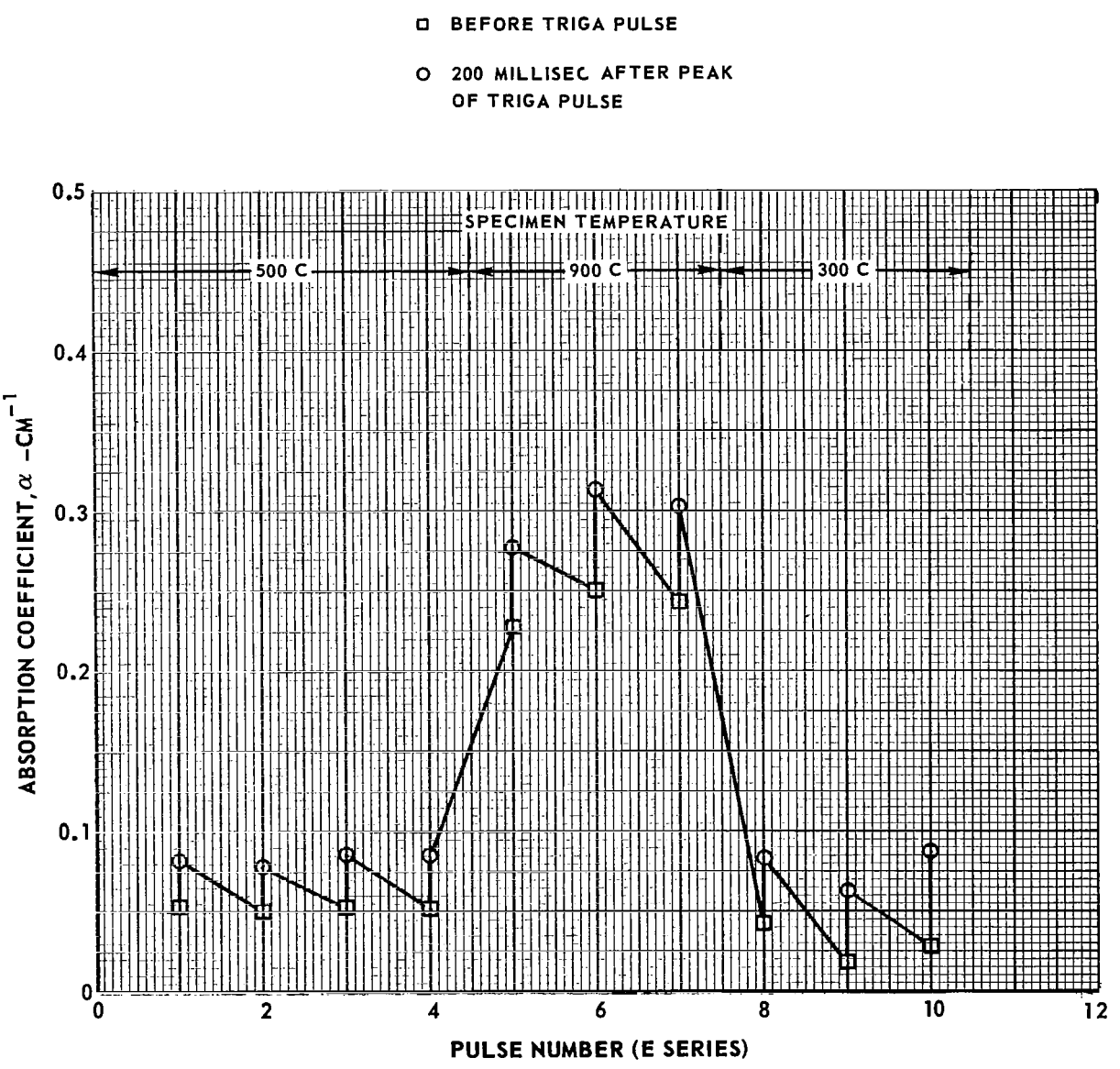

EFFECT OF SPECIMEN TEMPERATURE ON ABSORPTION COEFFICIENTS MEASURED BEFORE TRIGA PULSES FOR SERIES B THROUGH E

WAVELENGTH, $\lambda = 0.215$ MICRON

SYMBOL	RUN SERIES
◇	B
□	C
△	D
○	E

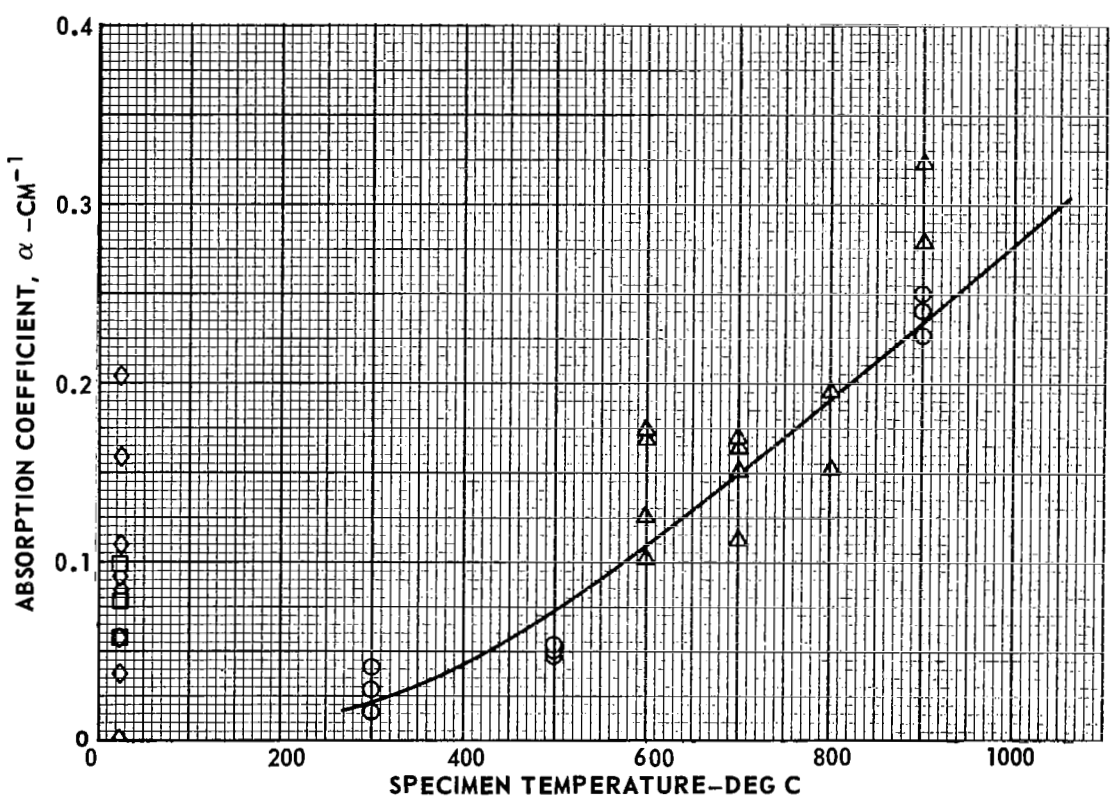

FIG. 19

TRANSMISSIVITY DURING RUNS D–1 THROUGH D–4 AT 700 C FOR TIMES UP TO 160 MILLISEC AFTER TRIGA PULSE

SPECIMEN SC 62–4

WAVELENGTH, λ = 0.215 MICRON

SYMBOL	RUN	$(I/I_0)_{REF}$	FRACTIONAL BYPASS CORRECTION (I/I_0) AT $t = 0$
○	D–1	0.492	0.355
△	D–2	0.391	0.497
□	D–3	0.359	0.523
◇	D–4	0.352	0.494

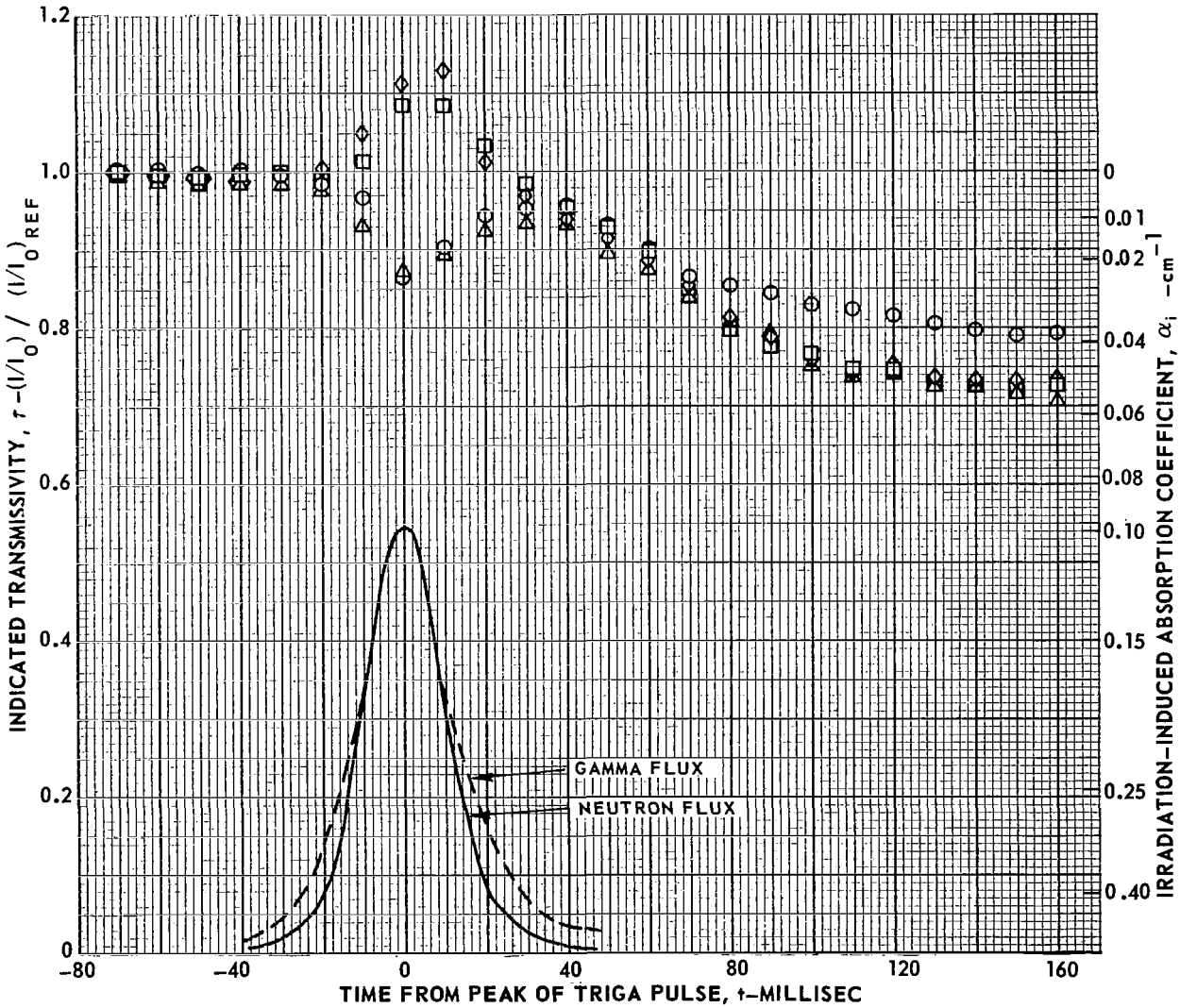

TRANSMISSIVITY DURING RUNS D–1 THROUGH D–4 AT 700 C FOR TIMES LONGER THAN 100 MILLISEC AFTER TRIGA PULSE

SPECIMEN SC 62–4

WAVELENGTH, λ = 0.215 MICRON

SYMBOL	RUN	$(I/I_0)_{REF}$
○	D–1	0.492
△	D–2	0.391
□	D–3	0.359
◇	D–4	0.352

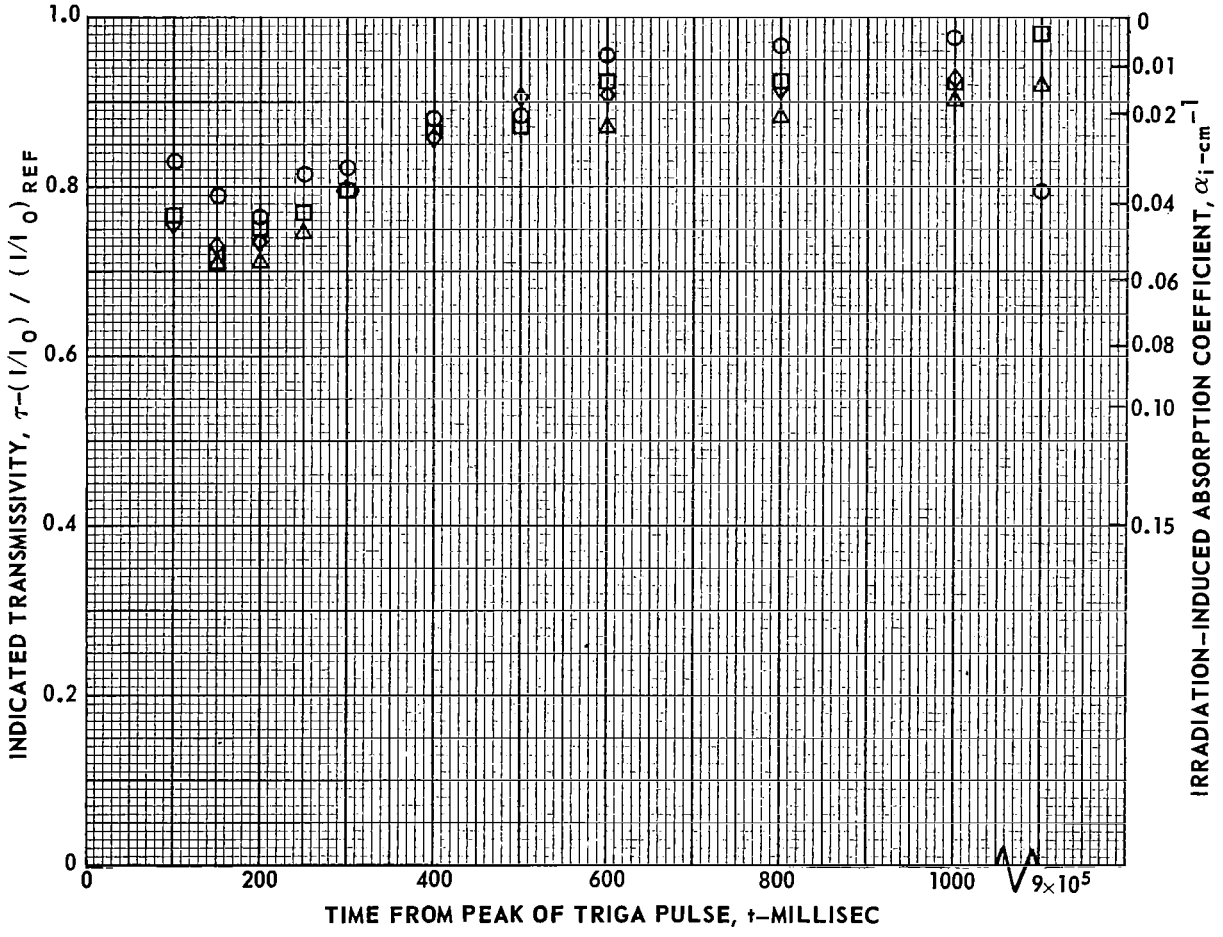

FIG. 21

TRANSMISSIVITY DURING RUNS D–5 AND D–6 AT 800 C FOR TIMES UP TO 160 MILLISEC AFTER TRIGA PULSE

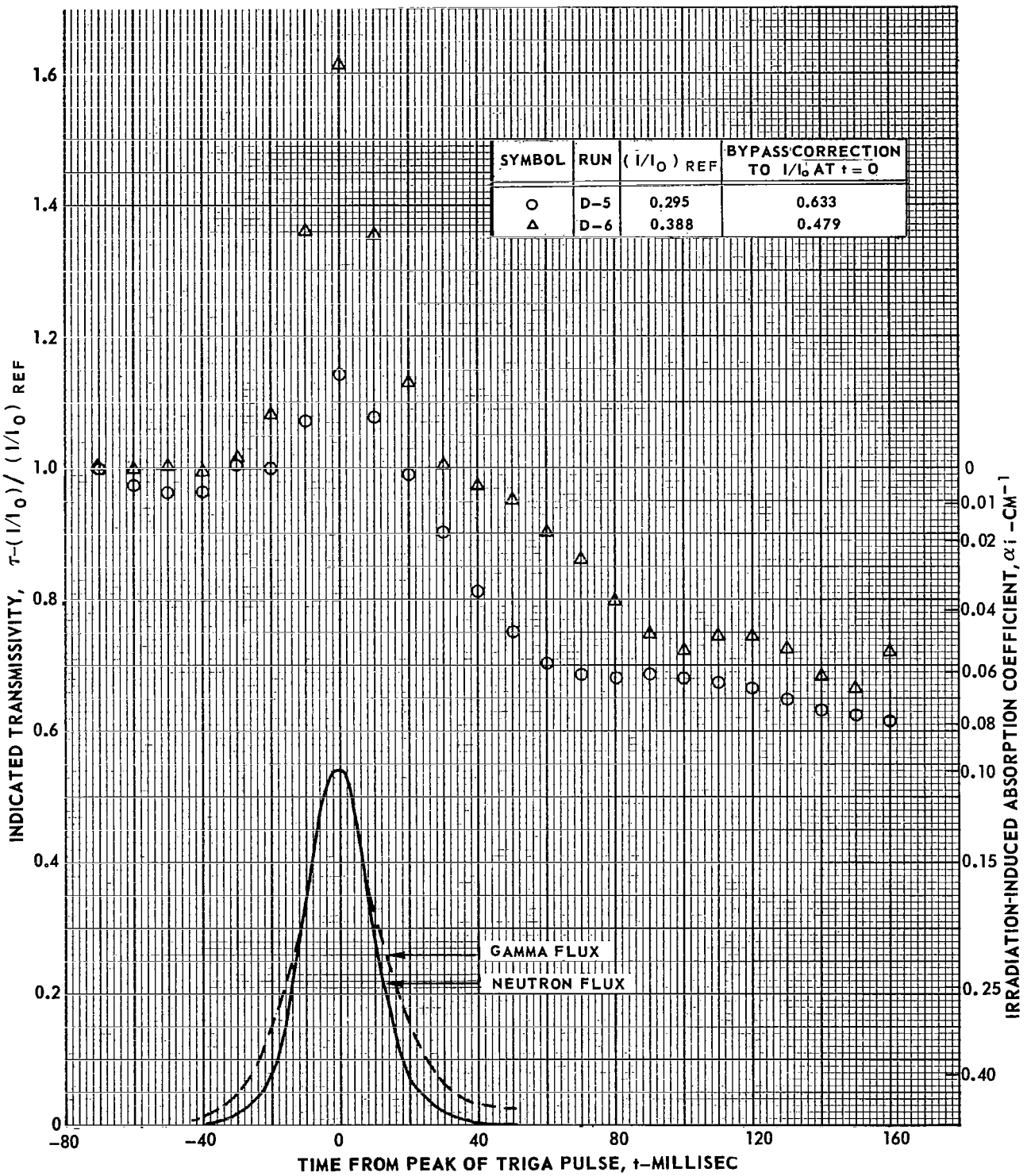

FIG. 22

TRANSMISSIVITY DURING RUNS D–5 AND D–6 AT 800 C FOR TIMES LONGER THAN 100 MILLISEC AFTER TRIGA PULSE

SPECIMEN SC 62–4

WAVELENGTH, λ = 0.215 MICRON

SYMBOL	RUN	$(I/I_0)_{REF}$
○	D–5	0.295
△	D–6	0.388

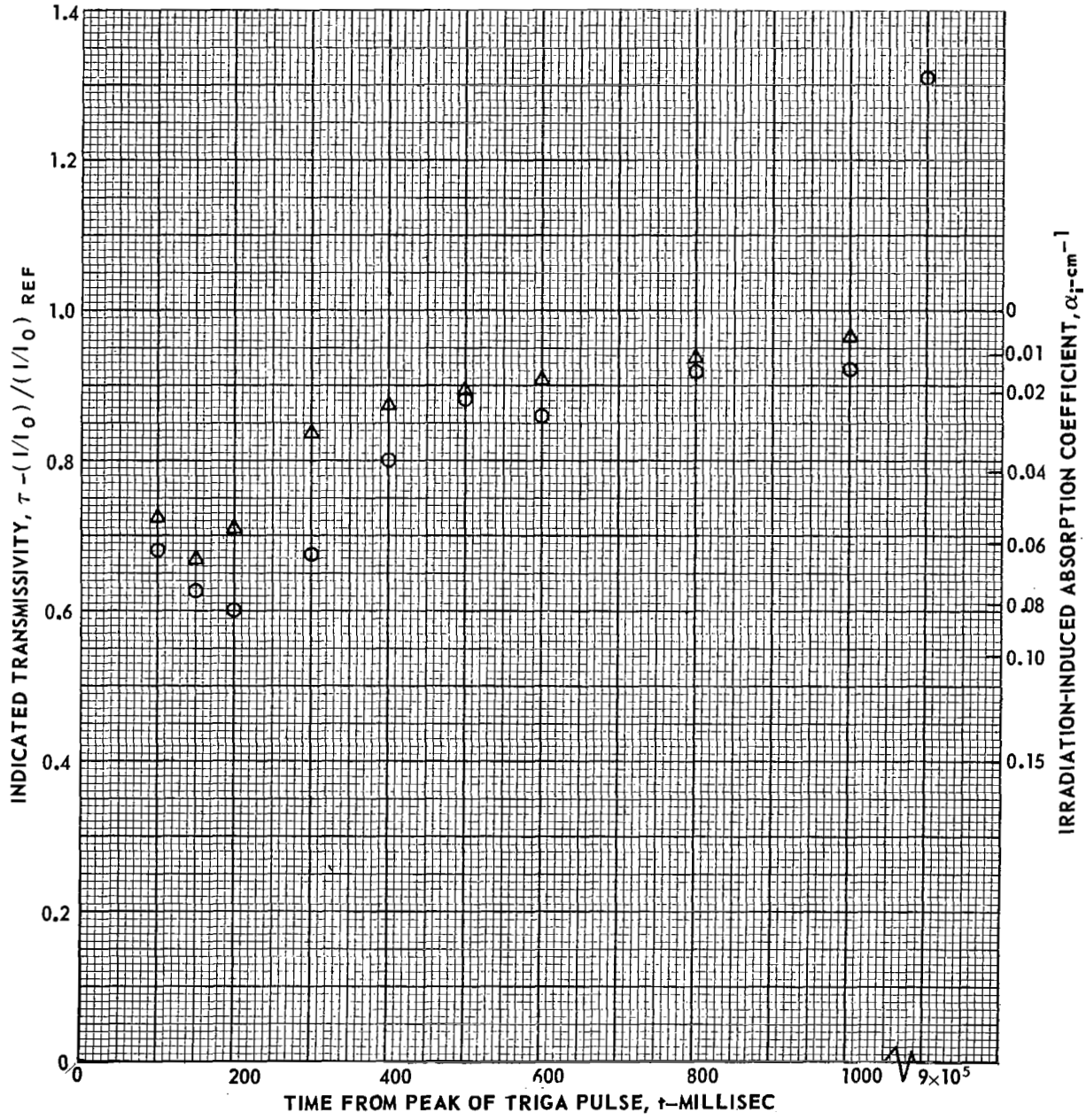

FIG. 23

TRANSMISSIVITY DURING RUNS D–7 AND D–8 AT 900 C FOR TIMES UP TO 160 MILLISEC AFTER TRIGA PULSE

SPECIMEN SC 62–4 WAVELENGTH, λ = 0.215 MICRON

SYMBOL	RUN	$(I/I_0)_{REF}$	FRACTIONAL BYPASS CORRECTION TO I/I_0 AT t= 0
○	D–7	0.134	1.36
△	D–8	0.177	1.11

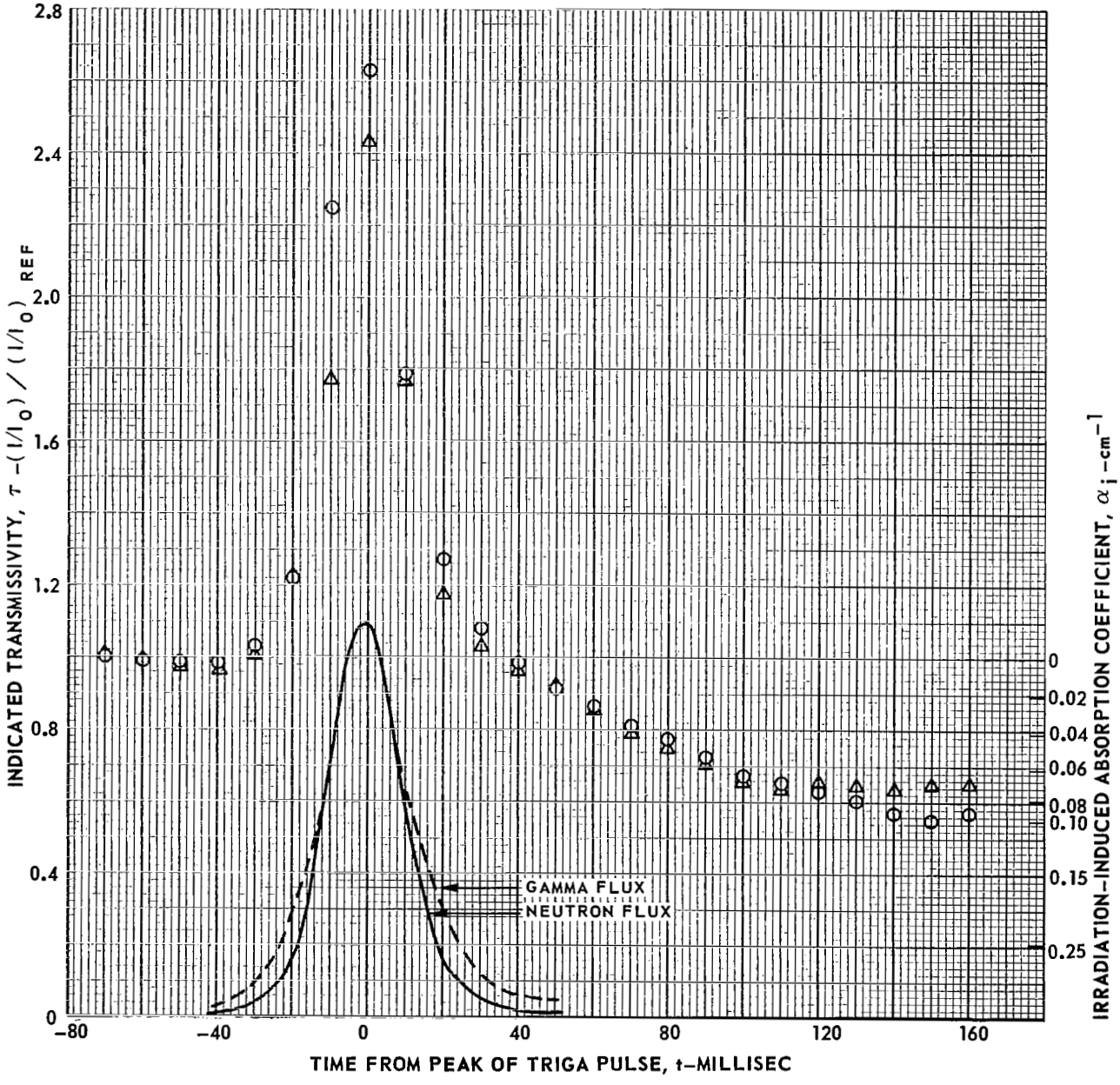

FIG. 24

TRANSMISSIVITY DURING RUNS D–7 AND D–8 AT 900 C FOR TIMES LONGER THAN 100 MILLISEC AFTER TRIGA PULSE

SPECIMEN SC 62–4 WAVELENGTH, $\lambda = 0.215$ MICRONS

SYMBOL	RUN	$(I/I_0)_{REF}$
○	D–7	0.134
□	D–8	0.177

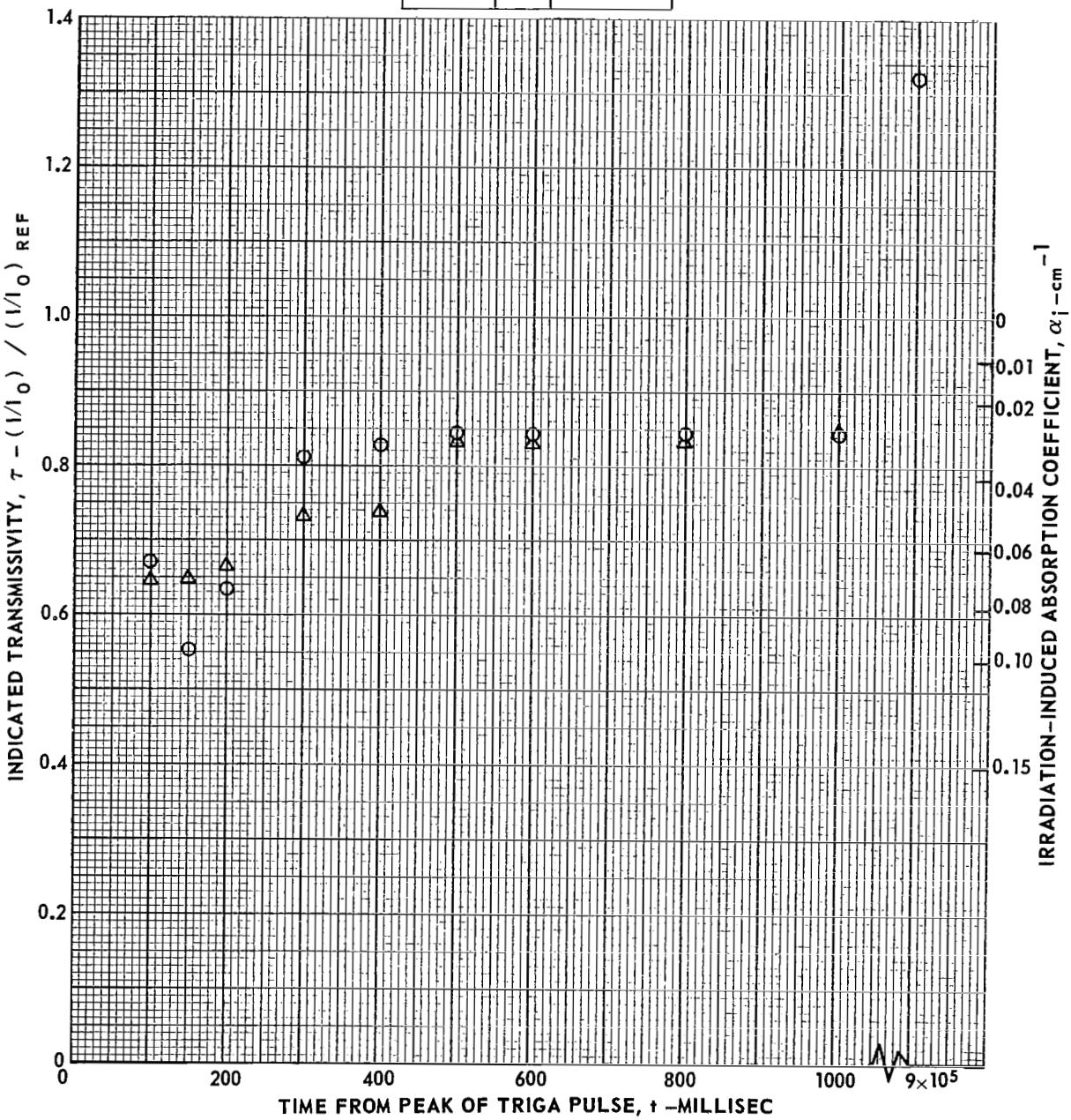

TRANSMISSIVITY DURING RUNS D–9 THROUGH D–12 AT 600 C FOR TIMES UP TO 200 MILLISEC AFTER TRIGA PULSE

SYMBOL	RUN	$(I/I_0)_{REF}$	FRACTIONAL BYPASS CORRECTION TO I/I_0 AT $t=0$
◇	D–9	0.459	0.491
○	D–10	0.531	0.414
□	D–11	0.340	0.568
△	D–12	0.345	0.568

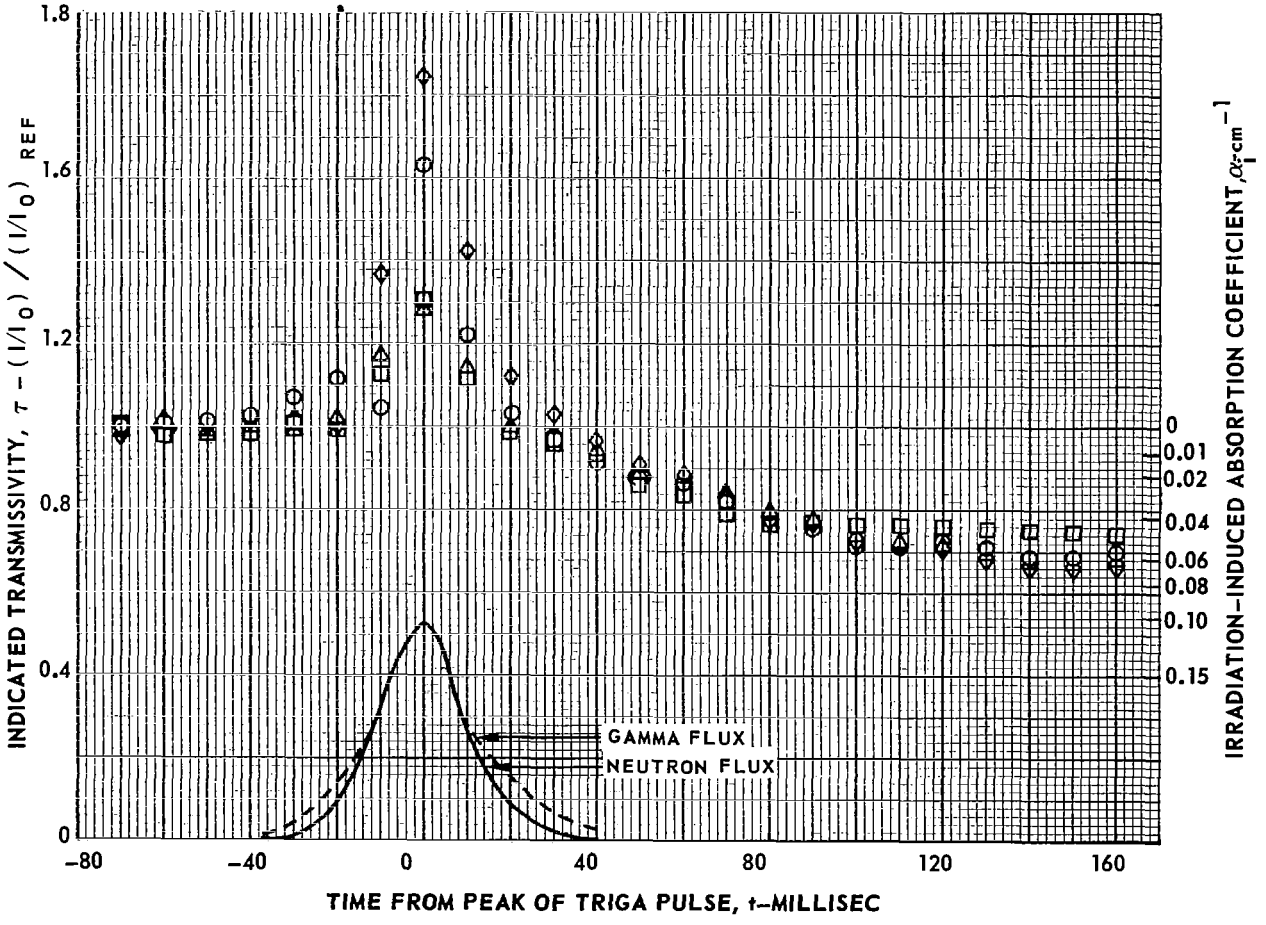

FIG. 26

TRANSMISSIVITY DURING RUNS D–9 THROUGH D–12 AT 600 C FOR TIMES LONGER THAN 100 MILLISEC AFTER TRIGA PULSE

SPECIMEN SC 62 – 4

WAVELENGTH, λ = 0.215 MICRON

SYMBOL	RUN	$(I/I_0)_{REF}$
◇	D–9	0.459
○	D–10	0.531
□	D–11	0.340
△	D–12	0.345

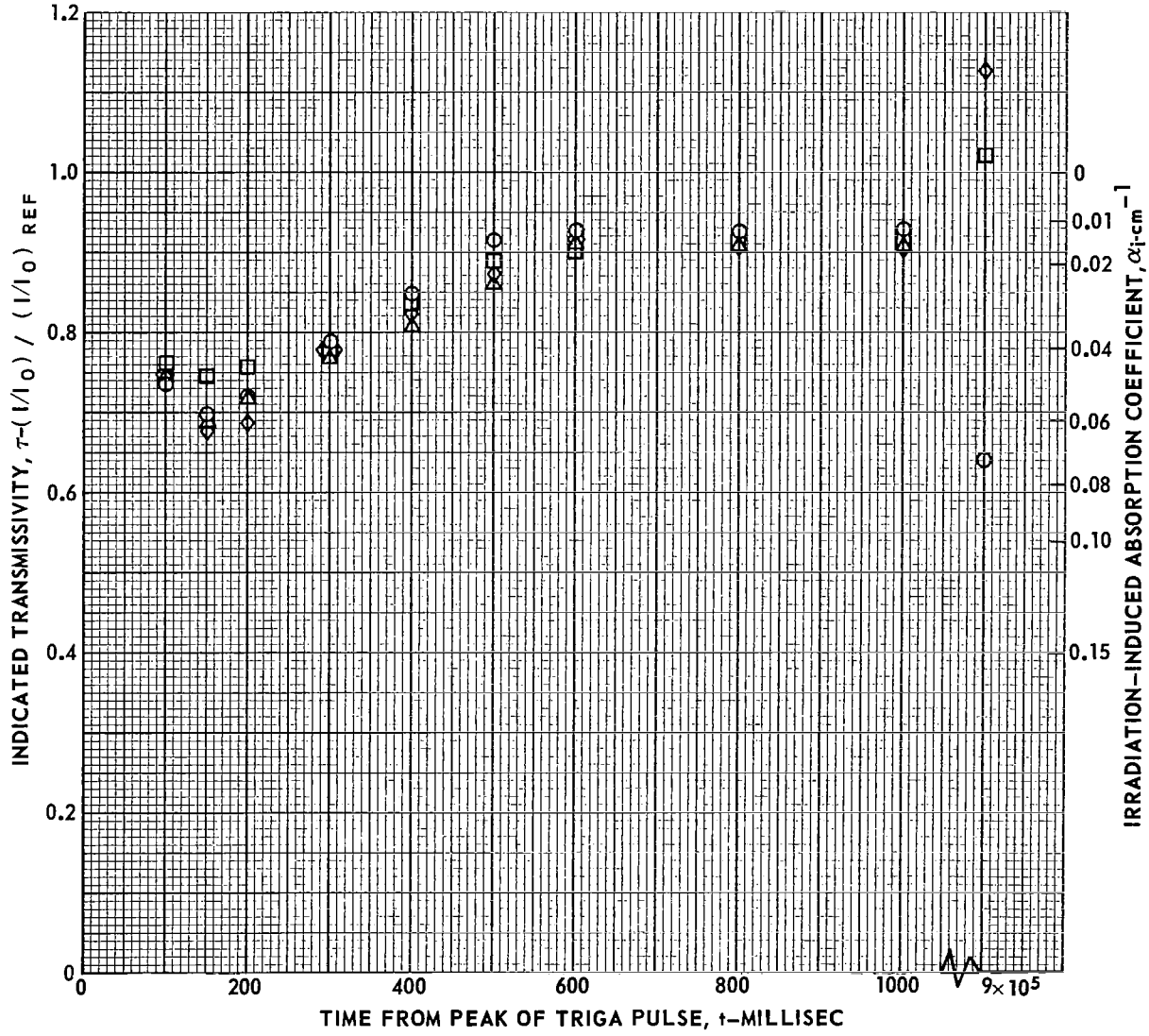

FIG. 27

TRANSMISSIVITY DURING RUNS E–1 THROUGH E–4 AT 500 C FOR TIMES UP TO 160 MILLISEC AFTER TRIGA PULSE

SPECIMEN SC 62–5

WAVELENGTH, λ = 0.215 MICRON

SYMBOL	RUN	$(I/I_0)_{REF}$	FRACTIONAL BYPASS CORRECTION TO I/I_0 AT $t = 0$
○	E–1	0.725	0.080
□	E–2	0.738	0.086
△	E–3	0.725	0.085
◇	E–4	0.718	0.087

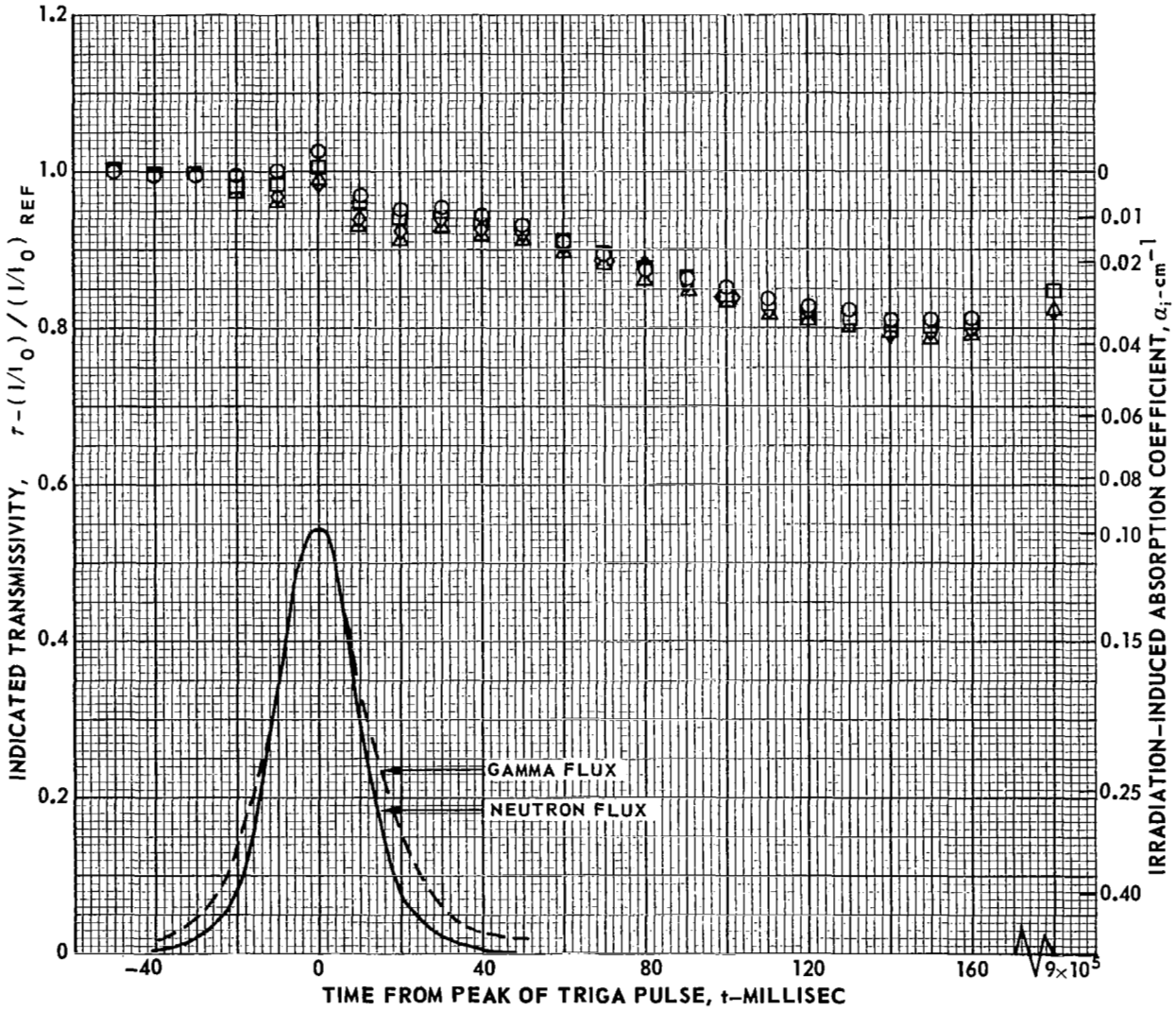

FIG. 28

TRANSMISSIVITY DURING RUNS E-1 THROUGH E-4 AT 500 C FOR TIMES LONGER THAN 100 MILLISEC AFTER TRIGA PULSE

SPECIMEN SC 62-5

WAVELENGTH, λ= 0.215 MICRON

SYMBOL	RUN	$(I/I_0)_{REF}$
○	E-1	0.725
□	E-2	0.738
△	E-3	0.725
◇	E-4	0.718

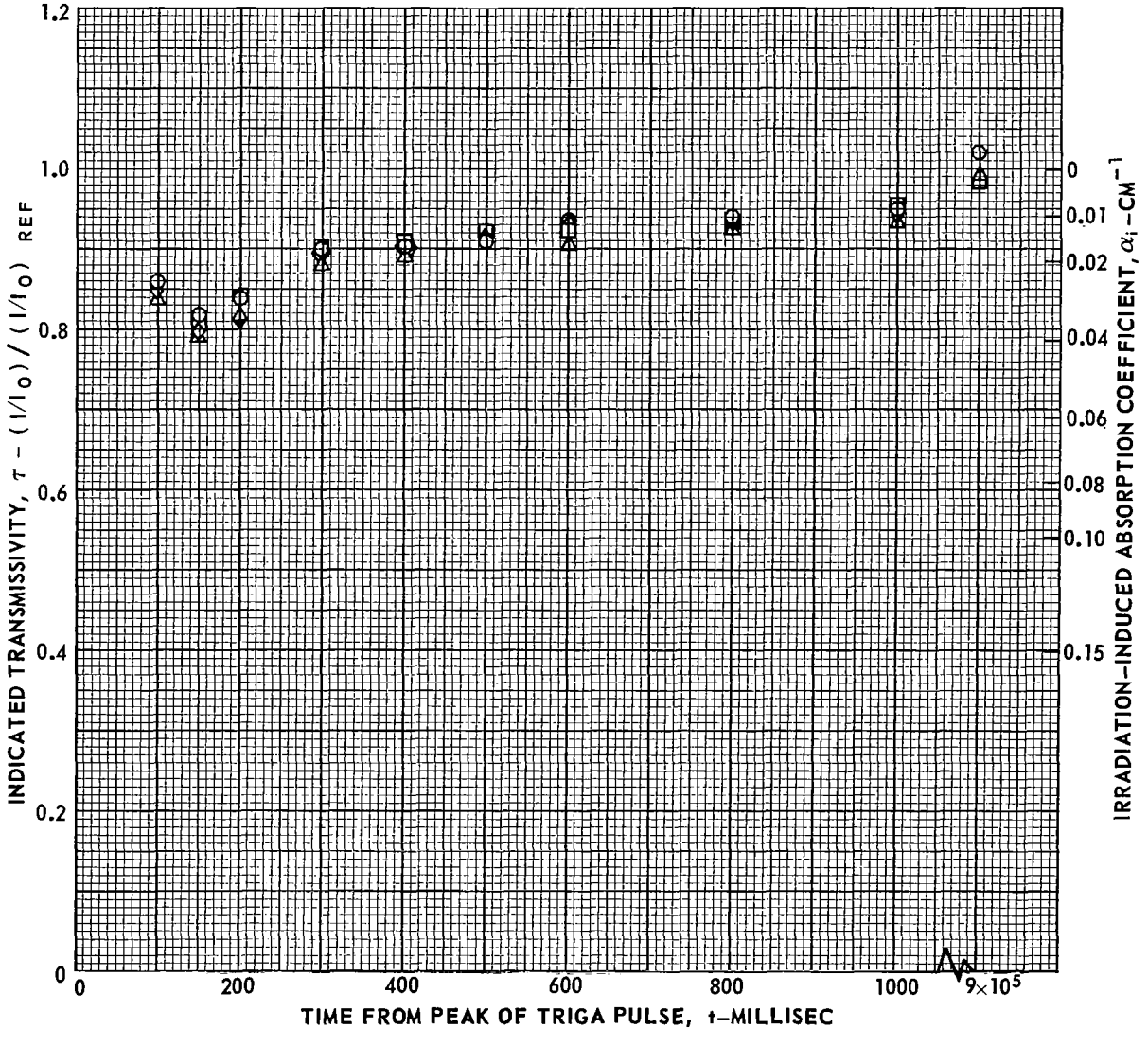

FIG. 29

TRANSMISSIVITY DURING RUNS E–5 THROUGH E–7 AT 900 C FOR TIMES UP TO 160 MILLISEC AFTER TRIGA PULSE

SPECIMEN SC 62–5

WAVELENGTH, λ = 0.215 MICRON

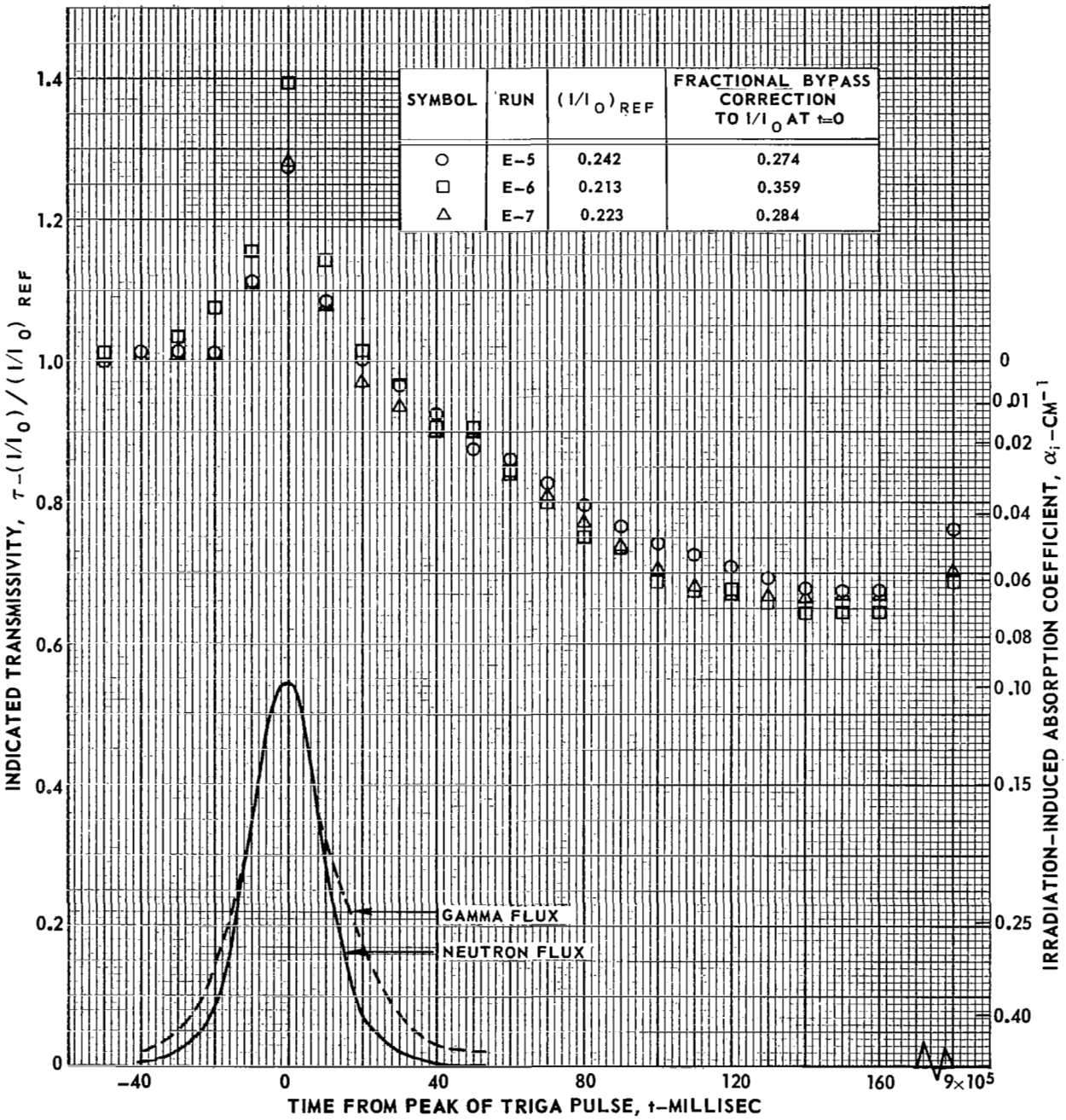

FIG. 30

TRANSMISSIVITY DURING RUNS E–5 THROUGH E–7 AT 900 C FOR TIMES LONGER THAN 100 MILLISEC AFTER TRIGA PULSE

SPECIMEN SC 62–5

WAVELENGTH, λ = 0.215 MICRON

SYMBOL	RUN	$(I/I_0)_{REF}$
○	E–5	0.242
□	E–6	0.213
△	E–7	0.223

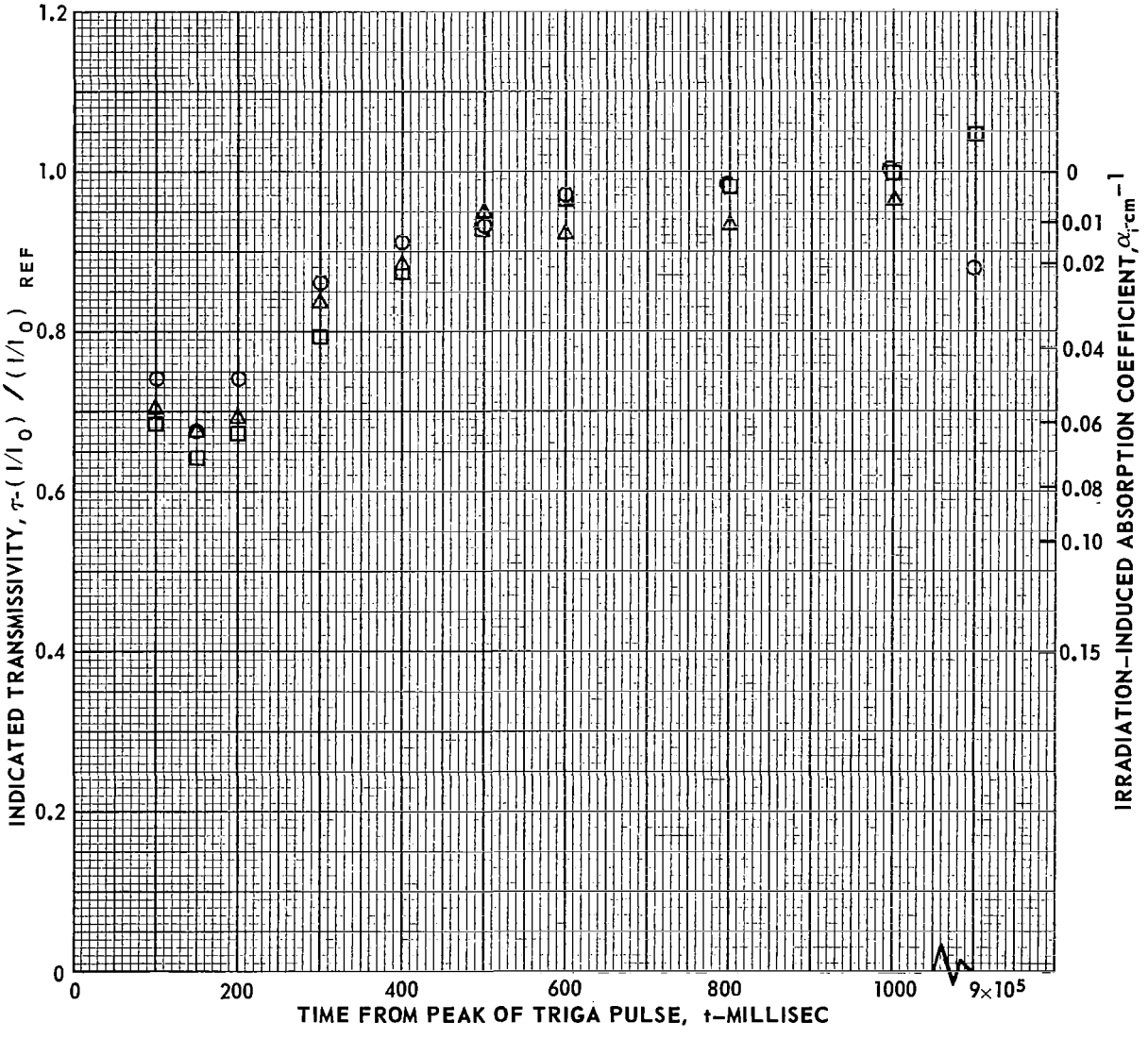

TRANSMISSIVITY DURING RUNS E-8 THROUGH E-10 AT 300 C FOR TIMES UP TO 160 MILLISEC AFTER TRIGA PULSE

SPECIMEN SC 62-5

WAVELENGTH, λ = 0.215 MICRON

SYMBOL	RUN	$(I/I_0)_{REF}$	FRACTIONAL BYPASS CORRECTION TO I/I_0 AT $t = 0$
○	E-8	0.774	0.081
□	E-9	0.894	0.080
△	E-10	0.835	0.088

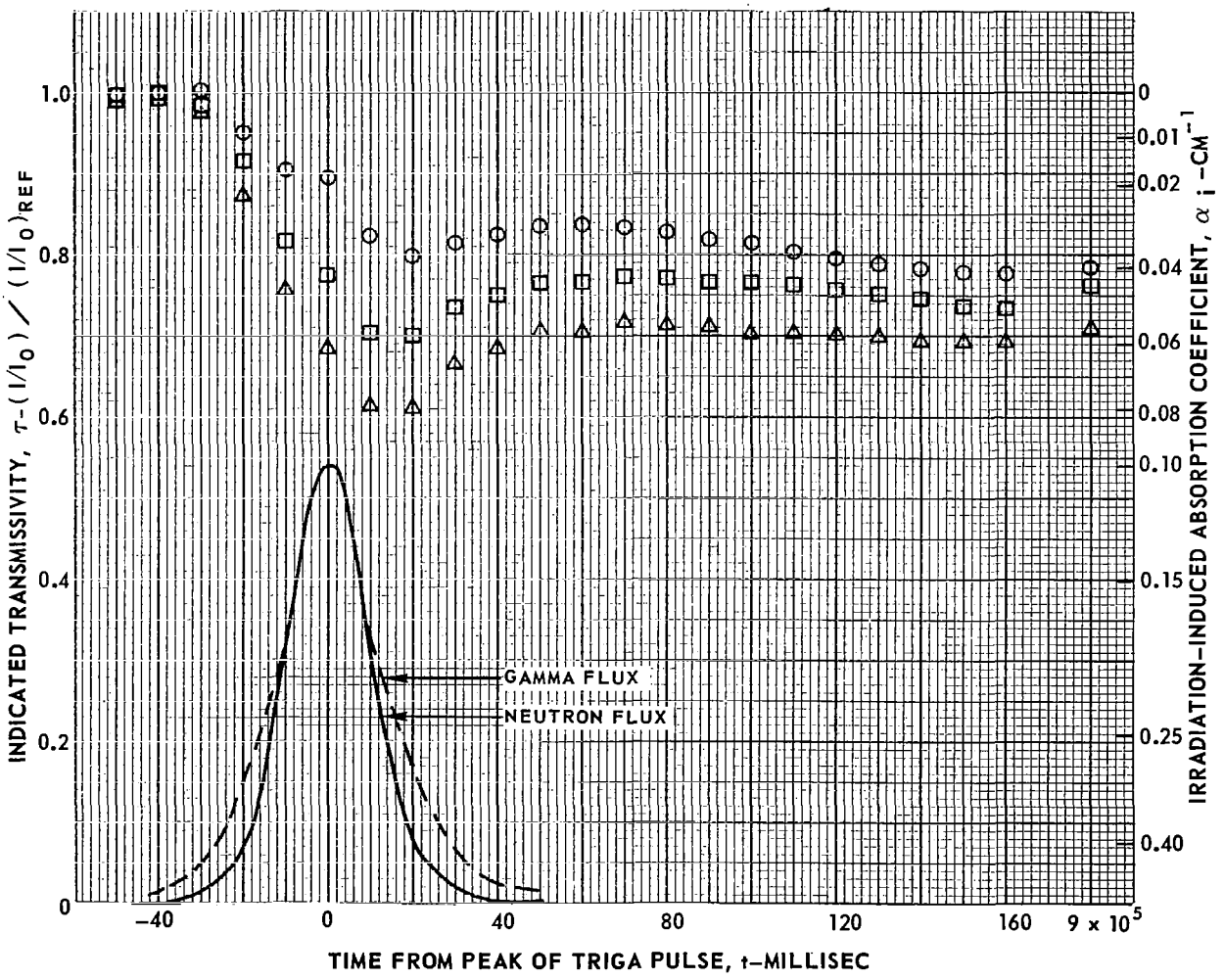

TRANSMISSIVITY DURING RUNS E–8 THROUGH E–10 AT 300 C FOR TIMES LONGER THAN 100 MILLISEC AFTER TRIGA PULSE

SPECIMEN SC 62–5

WAVELENGTH, $\lambda = 0.215$ MICRON

SYMBOL	RUN	$(I/I_0)_{REF}$
○	E–8	0.774
□	E–9	0.894
△	E–10	0.835

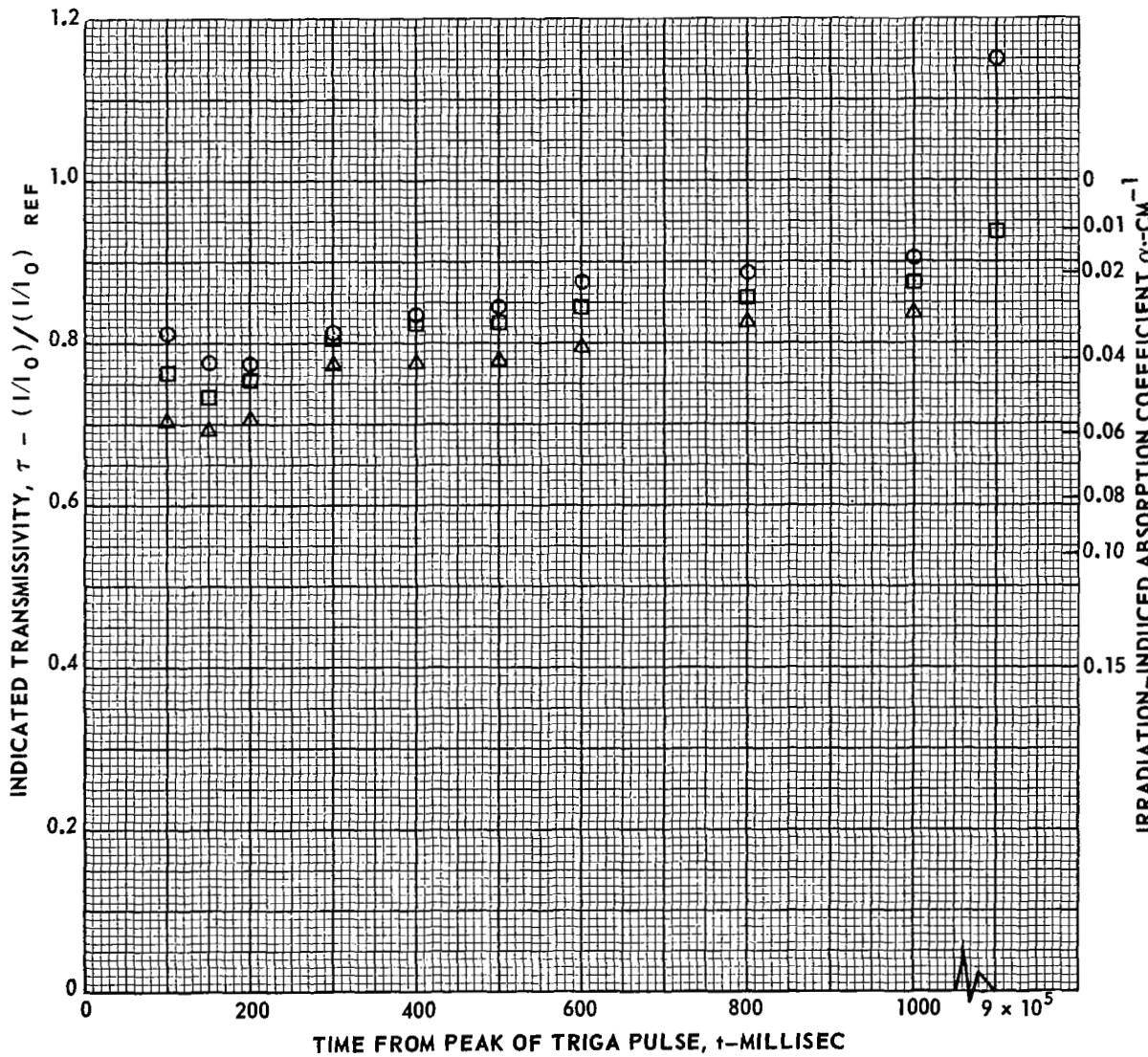

FIG. 33

COMPARISON OF TRANSMISSIVITIES AT DIFFERENT TEMPERATURES

WAVELENGTH, λ = 0.215 MICRON

SYMBOL	SPECIMEN	RUN	TEMPERATURE
◇	SC 62-2	B-1	AMBIENT
△	SC 62-5	E-8	300 C
○	SC 62-5	E-1	500 C
□	SC 62-5	E-5	900 C

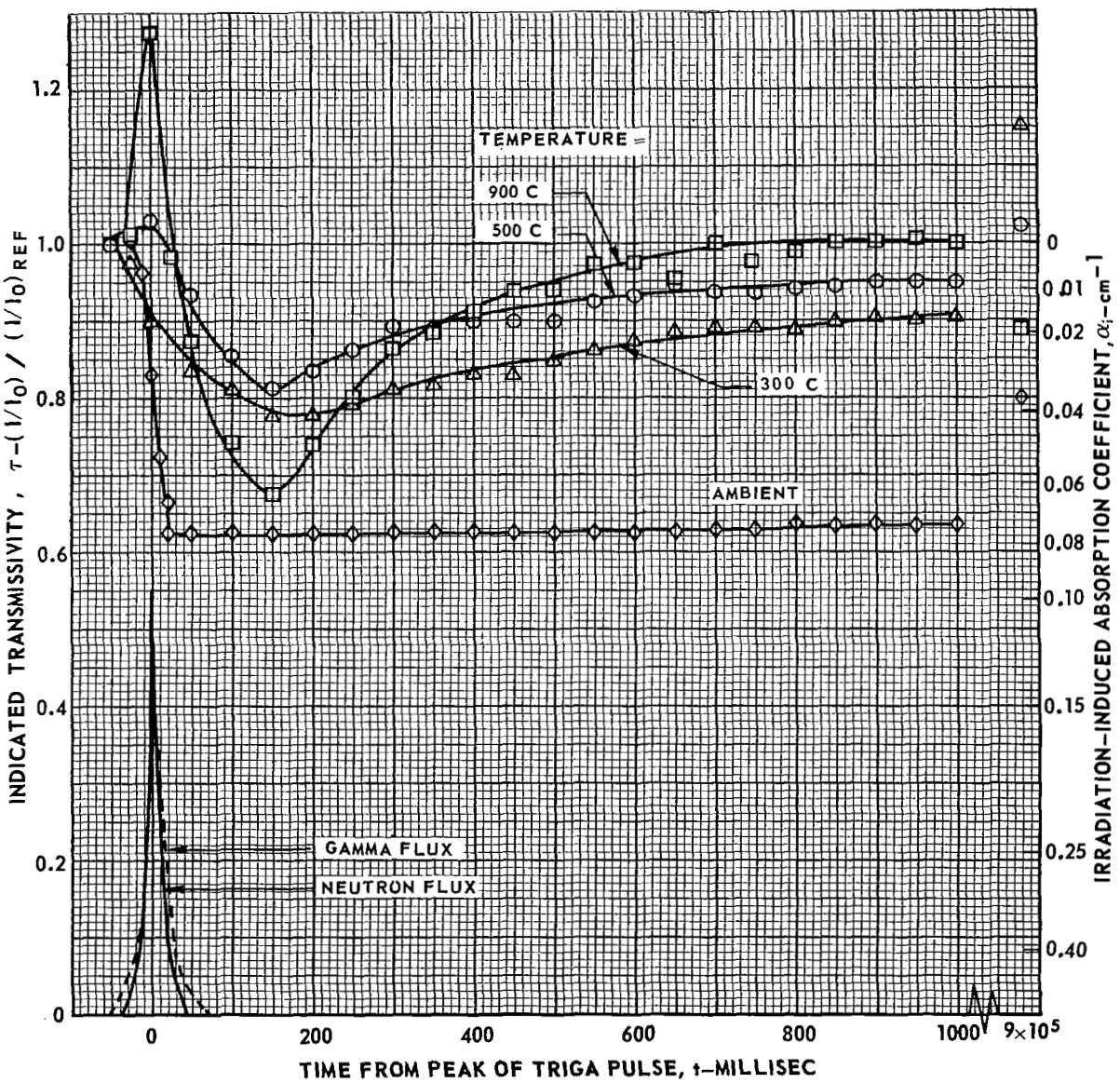

SEMI-LOGARITHMIC DECAY OF ABSORPTIVITY FOLLOWING RUNS D-1 THROUGH D-4 AT 700 C

SPECIMEN SC 62-4
WAVELENGTH λ = 0.215 MICRON

SYMBOL	RUN
○	D-1
□	D-2
◇	D-3
△	D-4

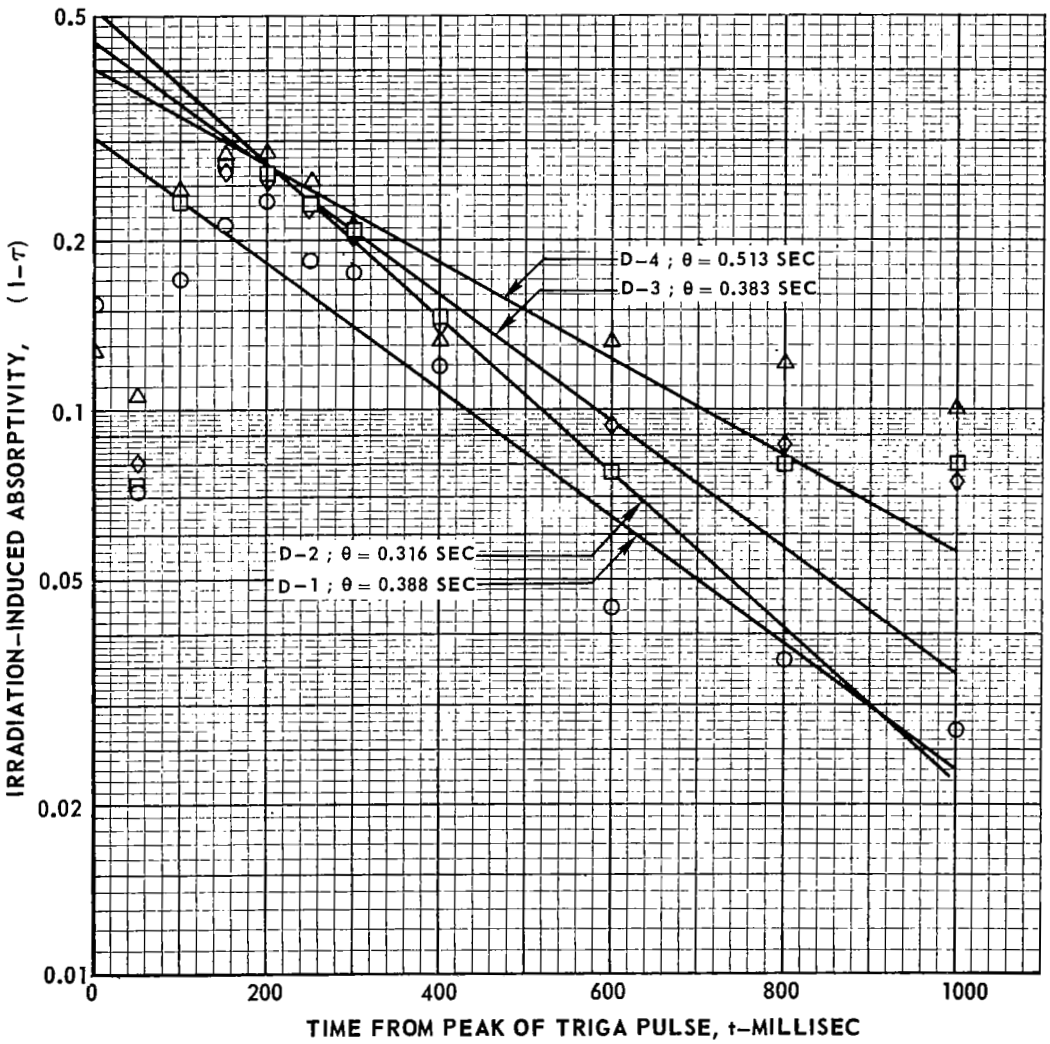

FIG. 35

SEMI–LOGARITHMIC DECAY OF ABSORPTIVITY FOLLOWING RUNS D–5 AND D–6 AT 800 C

SPECIMEN SC 62–4

WAVELENGTH, λ = 0.215 MICRON

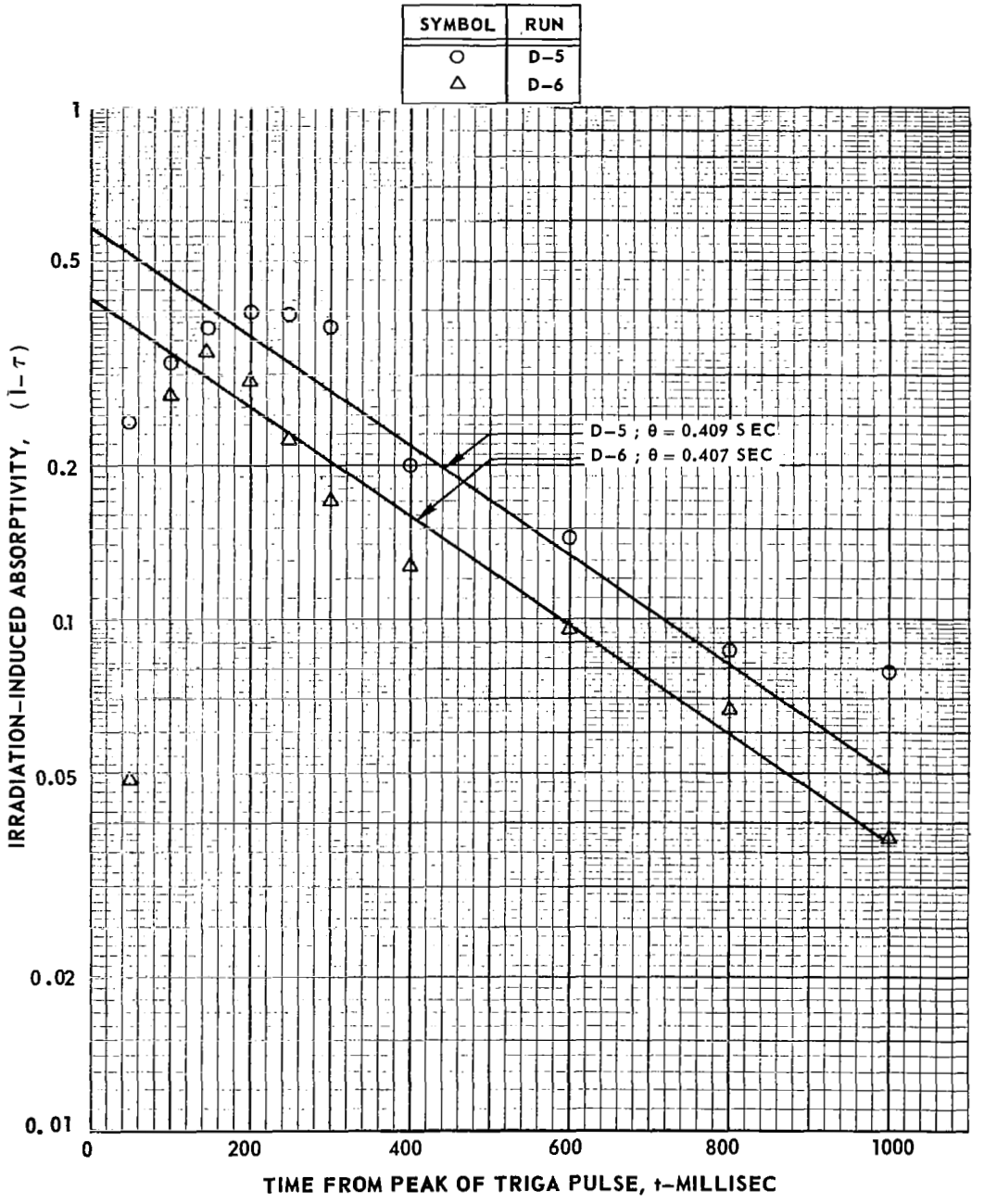

SEMI-LOGARITHMIC DECAY OF ABSORPTIVITY FOLLOWING RUNS D-7 AND D-8 AT 900 C

SPECIMEN SC 62-4

WAVELENGTH , λ = 0.215 MICRON

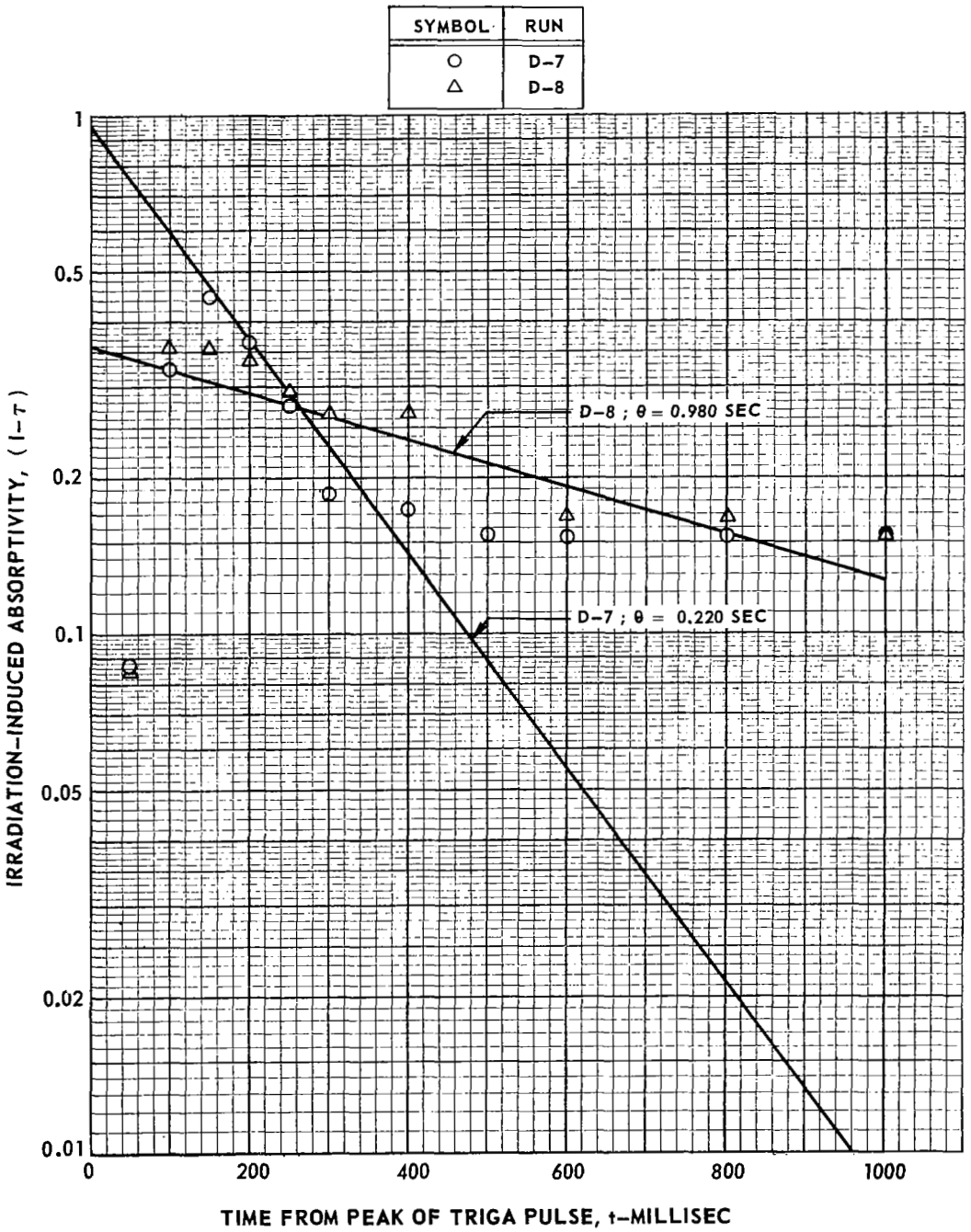

SEMI-LOGARITHMIC DECAY OF ABSORPTIVITY FOLLOWING RUNS D-9 AND D-12 AT 600 C

SPECIMEN SC 62-4
WAVELENGTH λ = 0.215 MICRON

SYMBOL	RUN
◇	D-9
○	D-10
□	D-11
△	D-12

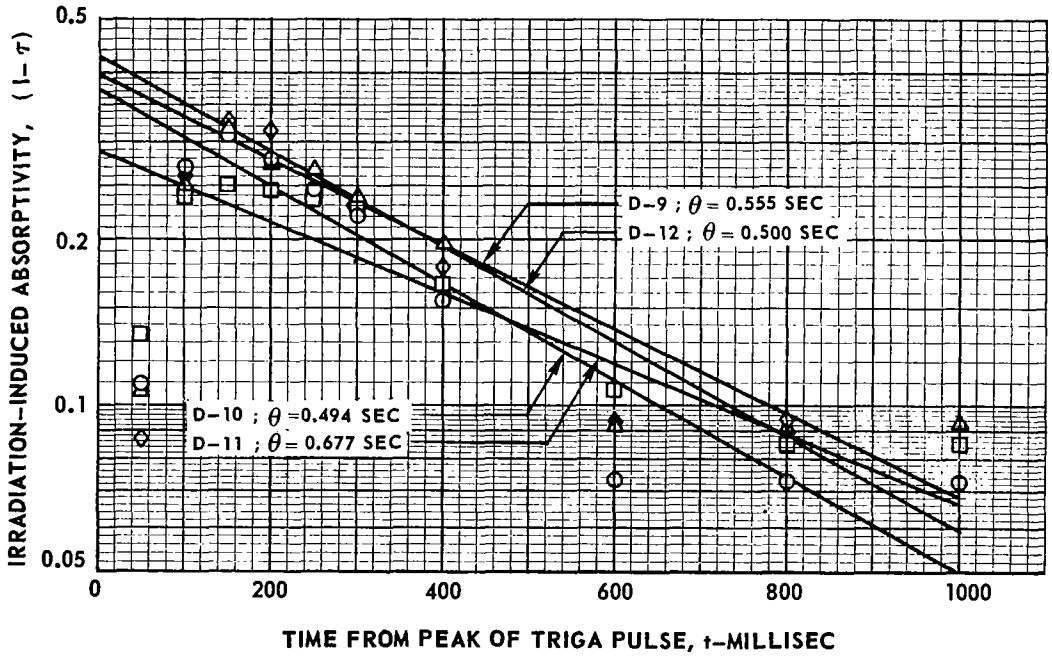

SEMI-LOGARITHMIC DECAY OF ABSORPTIVITY FOLLOWING RUNS E-1 THROUGH E-4 AT 500 C

SPECIMEN SC 62-5

WAVELENGTH, λ = 0.215 MICRON

SYMBOL	RUN
○	E - 1
□	E - 2
△	E - 3
◇	E - 4

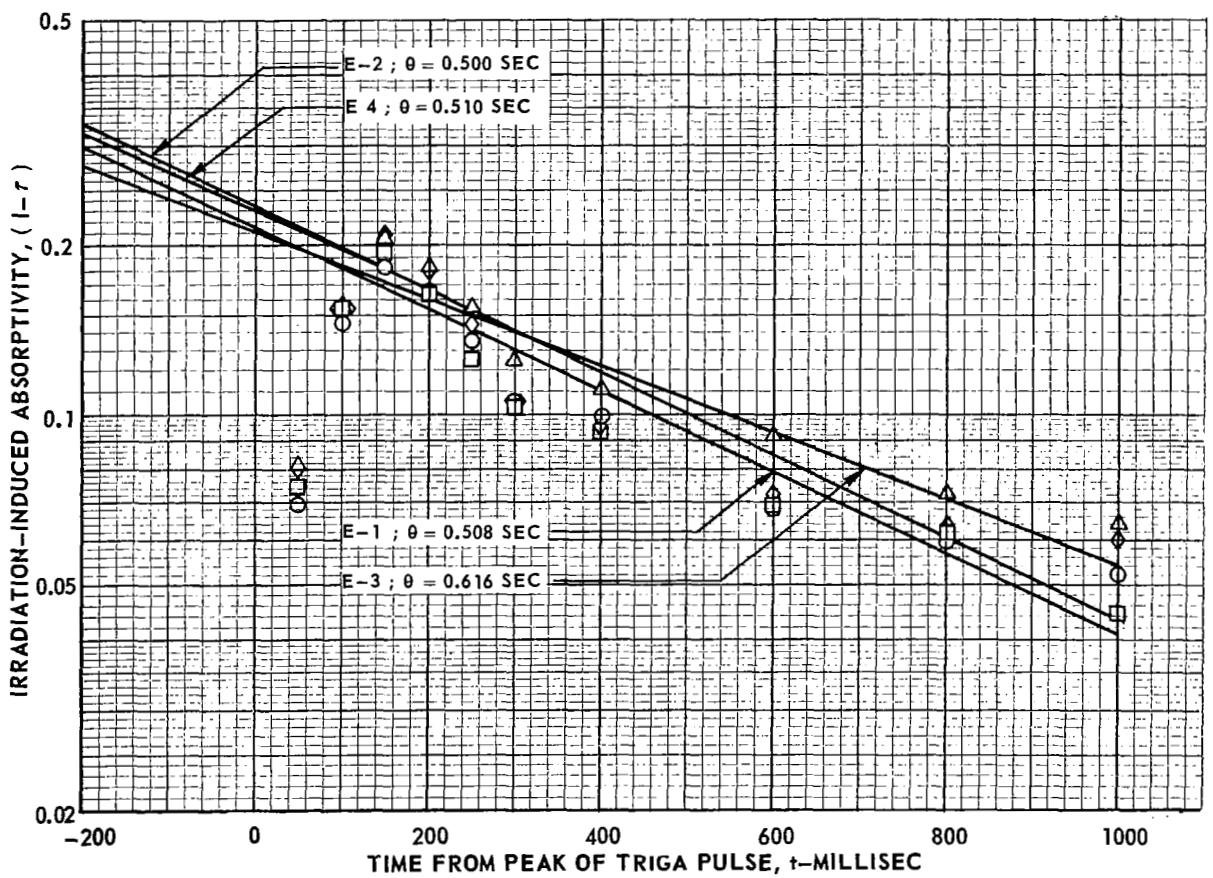

FIG. 39

SEMI-LOGARITHMIC DECAY OF ABSORPTIVITY FOLLOWING RUNS E-5 THROUGH E-7 AT 900 C

SPECIMEN SC 62-5

WAVELENGTH λ = 0.215 MICRON

SYMBOL	RUN
○	E-5
□	E-6
△	E-7

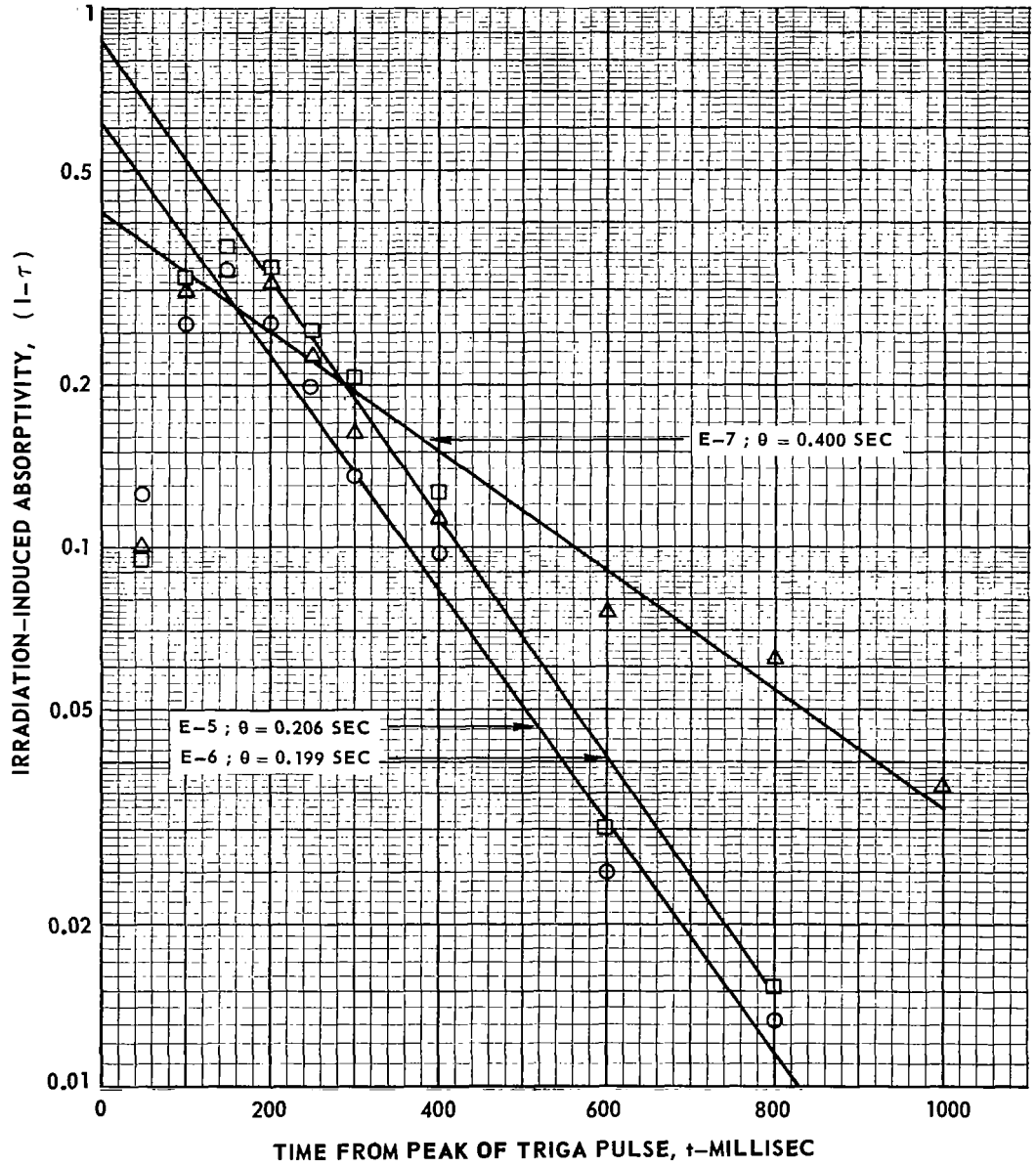

SEMI-LOGARITHMIC DECAY OF ABSORPTIVITY FOLLOWING RUNS E-8 THROUGH E-10 AT 300 C

SPECIMEN SC 62-5

WAVELENGTH, λ = 0.215 MICRON

SYMBOL	RUN
○	E-8
□	E-9
△	E-10

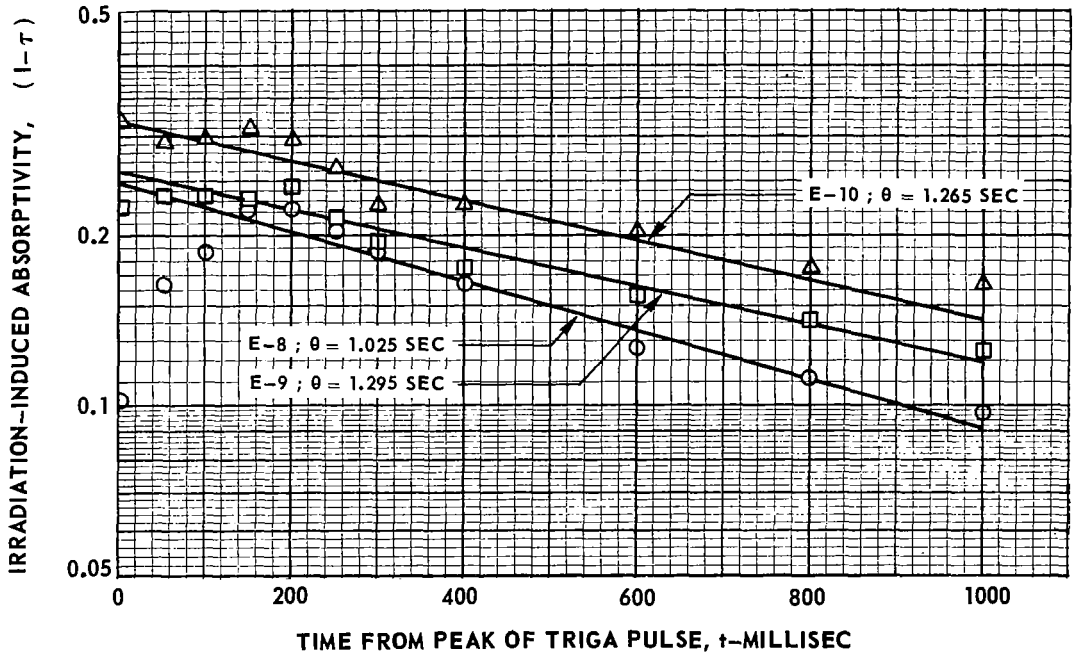

FIG. 41

VARIATION WITH TEMPERATURE OF REFERENCE IRRADIATION–INDUCED ABSORPTIVITY

WAVELENGTH, λ = 0.215 MICRON

SYMBOL	RUN
○	D–1 THROUGH D–12
□	E–1 THROUGH E–10

$(1-\tau)_0$ DEFINED AS VALUE OF STRAIGHT–LINE APPROXIMATION OF LOGARITHMIC DECAY CURVE AT $t = 0$ (SEE FIGS. 34–40)

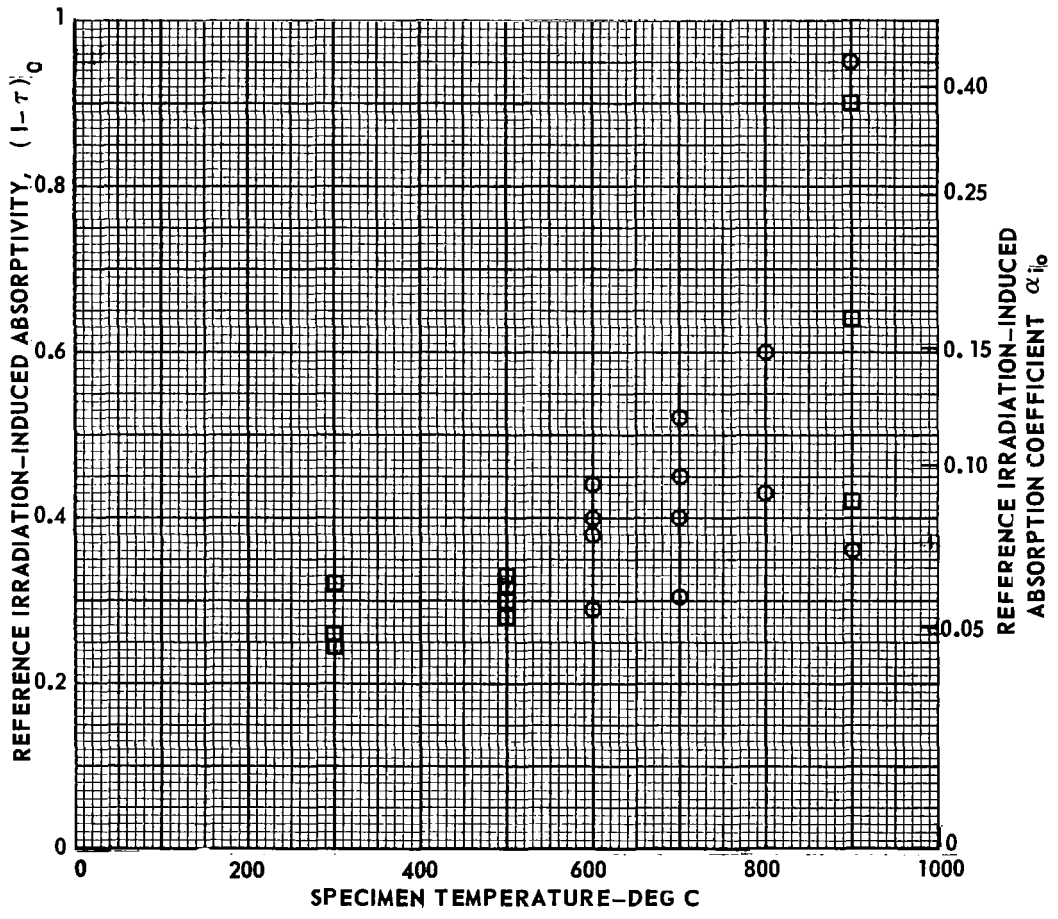

VARIATION WITH TEMPERATURE OF TIME CONSTANT FOR BLEACHING OF IRRADIATION-INDUCED ABSORPTIVITY

WAVELENGTH, λ = 0.215 MICRON

SYMBOL	RUNS
○	D-1 THROUGH D-12
□	E-1 THROUGH E-10

$$\frac{1-\tau}{(1-\tau)_0} = \frac{1}{e^{t/\theta}}$$

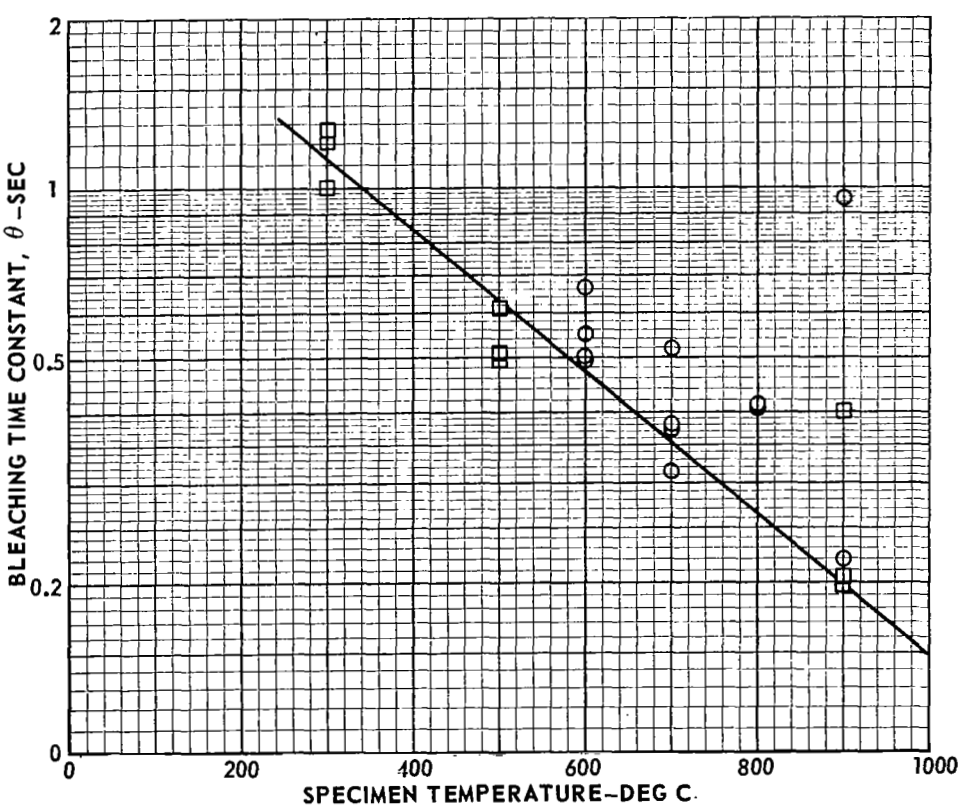

VARIATION WITH TEMPERATURE OF EQUILIBRIUM ABSORPTION COEFFICIENT

WAVELENGTH $\lambda = 0.215$ MICRON

SYMBOL	RUNS
○	D-1 THROUGH D-12
□	E-1 THROUGH E-10

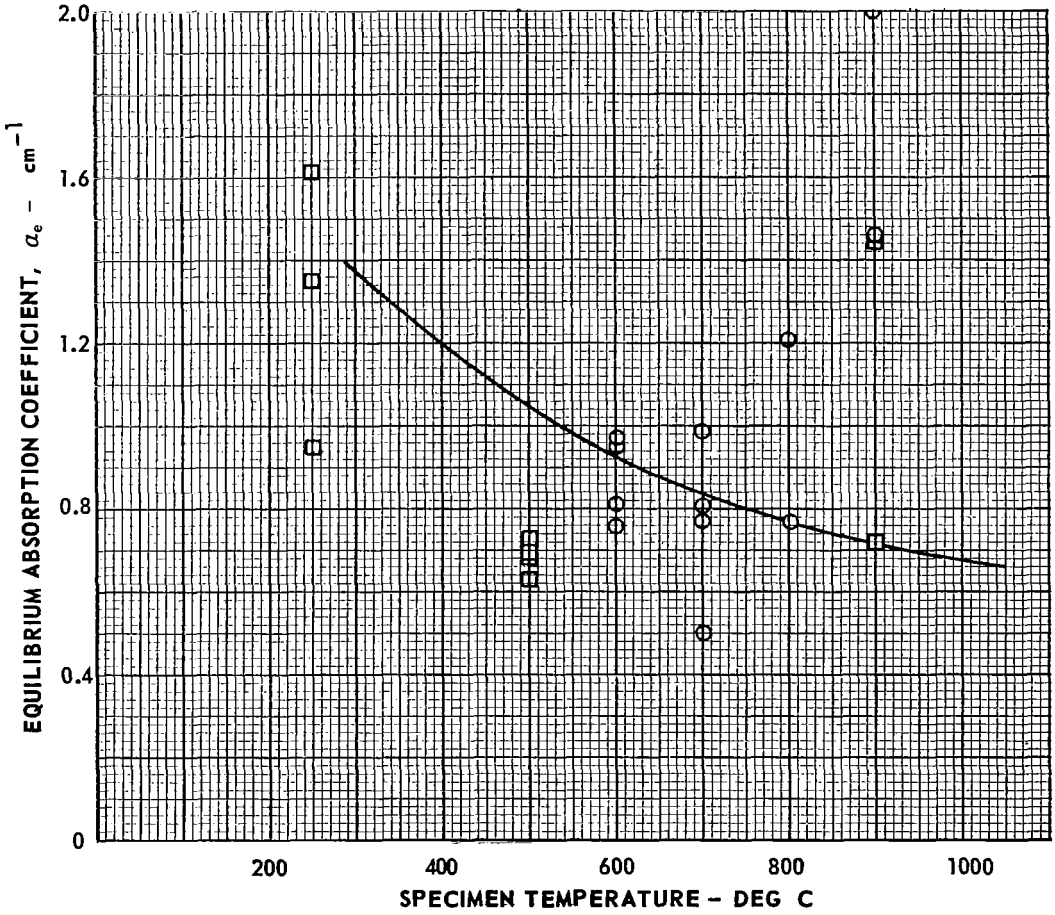

FIG. 44

TRANSMISSIVITY DURING RUNS E–12 AND E–16 AT WAVELENGTH OF 0.625 MICRON

SPECIMEN SC 62–5

WAVELENGTH, λ = 0.625 MICRON

SYMBOL	RUN	TEMPERATURE	$(I/I_0)_{REF}$	FRACTIONAL BYPASS CORRECTION TO I/I_0 AT t=0
○	E–12	66 C	2.15	0.01
◇	E–16	500 C	1.65	0.01

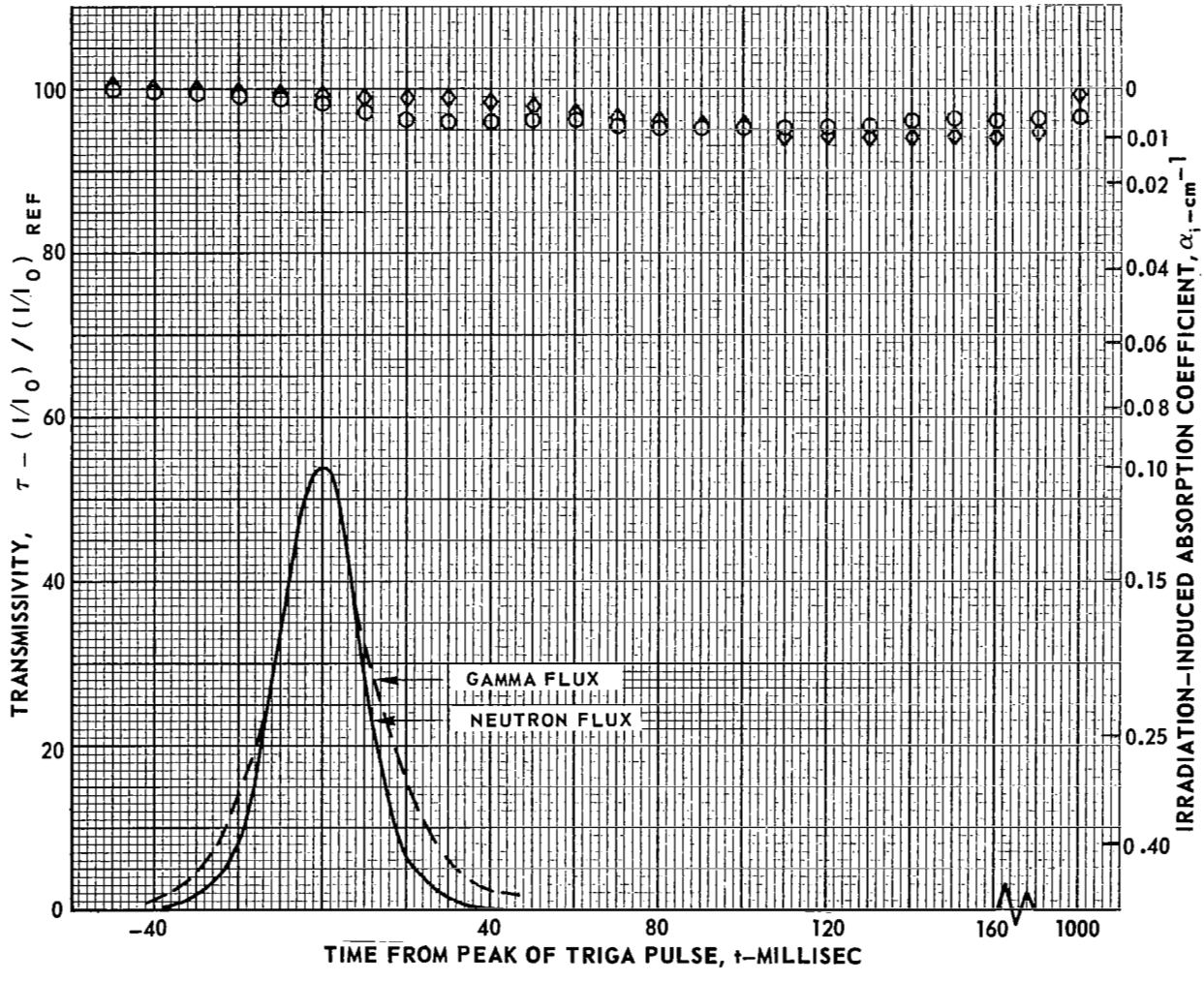

FIG. 45

TRANSMISSIVITY DURING RUN E-15 AT WAVELENGTH OF 1.0 MICRON

SPECIMEN SC 62-5

BYPASS CORRECTION ZERO

$(I/I_0)_{REF} = 1.73$

TEMPERATURE = AMBIENT

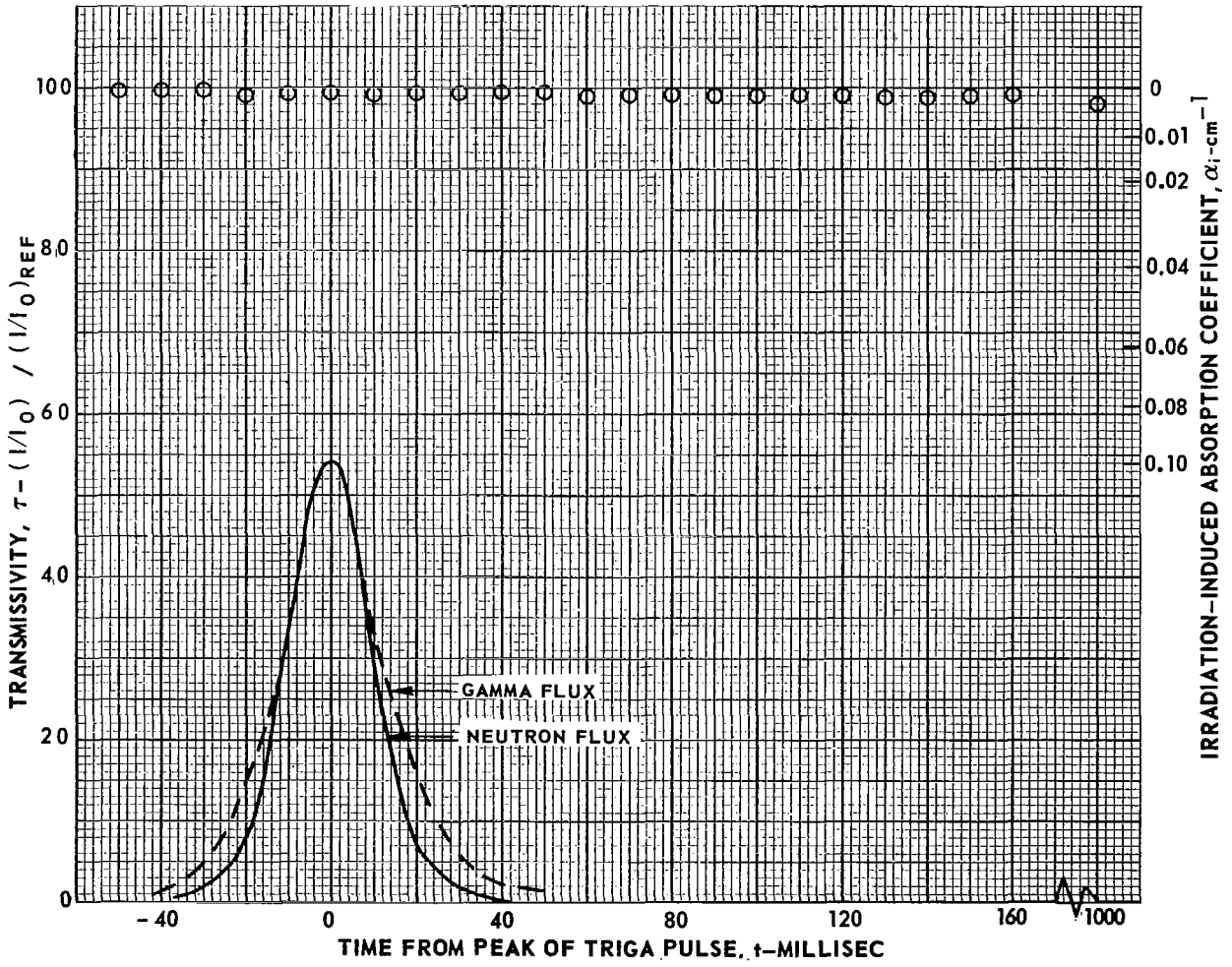

"The aeronautical and space activities of the United States shall be conducted so as to contribute . . . to the expansion of human knowledge of phenomena in the atmosphere and space. The Administration shall provide for the widest practicable and appropriate dissemination of information concerning its activities and the results thereof."

—NATIONAL AERONAUTICS AND SPACE ACT OF 1958

NASA SCIENTIFIC AND TECHNICAL PUBLICATIONS

TECHNICAL REPORTS: Scientific and technical information considered important, complete, and a lasting contribution to existing knowledge.

TECHNICAL NOTES: Information less broad in scope but nevertheless of importance as a contribution to existing knowledge.

TECHNICAL MEMORANDUMS: Information receiving limited distribution because of preliminary data, security classification, or other reasons.

CONTRACTOR REPORTS: Scientific and technical information generated under a NASA contract or grant and considered an important contribution to existing knowledge.

TECHNICAL TRANSLATIONS: Information published in a foreign language considered to merit NASA distribution in English.

SPECIAL PUBLICATIONS: Information derived from or of value to NASA activities. Publications include conference proceedings, monographs, data compilations, handbooks, sourcebooks, and special bibliographies.

TECHNOLOGY UTILIZATION PUBLICATIONS: Information on technology used by NASA that may be of particular interest in commercial and other non-aerospace applications. Publications include Tech Briefs, Technology Utilization Reports and Notes, and Technology Surveys.

Details on the availability of these publications may be obtained from:

SCIENTIFIC AND TECHNICAL INFORMATION DIVISION

NATIONAL AERONAUTICS AND SPACE ADMINISTRATION

Washington, D.C. 20546